

Activation of Histone Deacetylase-6 Induces Contractile Dysfunction Through Derailment of α -Tubulin Proteostasis in Experimental and Human Atrial Fibrillation

Deli Zhang, MSc; Chia-Tung Wu, MD; XiaoYan Qi, PhD; Roelien A.M. Meijering, MSc; Femke Hoogstra-Berends, BSc; Artavazd Tadevosyan, MSc; Günseli Cubukcuoglu Deniz, PhD; Serkan Durdu, MD, PhD; Ahmet Ruchan Akar, MD, FRCS (CTh); Ody C.M. Sibon, PhD; Stanley Nattel, MD; Robert H. Henning, MD, PhD; Bianca J.J.M. Brundel, PhD

Background—Atrial fibrillation (AF) is characterized by structural remodeling, contractile dysfunction, and AF progression. Histone deacetylases (HDACs) influence acetylation of both histones and cytosolic proteins, thereby mediating epigenetic regulation and influencing cell proteostasis. Because the exact function of HDACs in AF is unknown, we investigated their role in experimental and clinical AF models.

Methods and Results—Tachypacing of HL-1 atrial cardiomyocytes and *Drosophila* pupae hearts significantly impaired contractile function (amplitude of Ca^{2+} transients and heart wall contractions). This dysfunction was prevented by inhibition of HDAC6 (tubacin) and sirtuins (nicotinamide). Tachypacing induced specific activation of HDAC6, resulting in α -tubulin deacetylation, depolymerization, and degradation by calpain. Tachypacing-induced contractile dysfunction was completely rescued by dominant-negative HDAC6 mutants with loss of deacetylase activity in the second catalytic domain, which bears α -tubulin deacetylase activity. Furthermore, in vivo treatment with the HDAC6 inhibitor tubastatin A protected atrial tachypaced dogs from electric remodeling (action potential duration shortening, L-type Ca^{2+} current reduction, AF promotion) and cellular Ca^{2+} -handling/contractile dysfunction (loss of Ca^{2+} transient amplitude, sarcomere contractility). Finally, atrial tissue from patients with AF also showed a significant increase in HDAC6 activity and reduction in the expression of both acetylated and total α -tubulin.

Conclusions—AF induces remodeling and loss of contractile function, at least in part through HDAC6 activation and subsequent derailment of α -tubulin proteostasis and disruption of the cardiomyocyte microtubule structure. In vivo inhibition of HDAC6 protects against AF-related atrial remodeling, disclosing the potential of HDAC6 as a therapeutic target in clinical AF. (*Circulation*. 2014;129:346-358.)

Key Words: alpha-tubulin deacetylase ■ atrial fibrillation ■ *Drosophila* ■ epigenesis, genetic ■ HDAC6 protein, *Drosophila* ■ HDAC6 protein, human

Atrial fibrillation (AF) is the most common persistent clinical tachyarrhythmia and a significant contributor to cardiovascular morbidity and mortality.¹ AF is progressive in nature because of atrial remodeling, which provides a further substrate for the arrhythmia. Because the expansion of the AF substrate is not addressed by current drug therapies, the likelihood of conversion to sinus rhythm declines with persistence of the arrhythmia.¹ Thus, there is a need for treatments limiting or reversing the cellular substrates for AF, that is, the molecular changes that cause structural remodeling and drive the development and progression of the arrhythmia.²

Identification of druggable targets in these pathways is an initial step toward such “upstream therapy.”³

Clinical Perspective on p 358

Several observations suggest a prominent role for epigenetic regulation in the promotion of AF. Epigenetic regulation refers to processes that influence the packaging or processing of nuclear DNA, thus controlling the on/off states of multiple genes with discrete switches. Epigenetic regulation thus profoundly affects cellular proteostasis, that is, the homeostasis of protein production, degradation, and function.^{4,5} Derailment of

Received August 14, 2012; accepted October 2, 2013.

From the Departments of Clinical Pharmacology (D.Z., R.A.M.M., F.H.-B., R.H.H., B.J.J.M.B.) and Cell Biology (O.C.M.S.), University Medical Center Groningen, University of Groningen, Groningen, The Netherlands; Research Center and Department of Medicine, Montreal Heart Institute and Université de Montréal, Montreal, QB, Canada (C.T.W., X.Y.Q., A.T., S.N.); Chang-Gung Memorial Hospital and Chang-Gung University, Taoyuan, Taiwan, Republic of China (C.T.W.); Nyken BV, Groningen, The Netherlands (F.-H.B.); Ankara University Biotechnology Institute, Ankara, Turkey (G.C.D., S.D.); Ankara University Stem Cell Institute, Ankara, Turkey (G.C.D., S.D., A.R.A.); Department of Cardiovascular Surgery, Ankara University School of Medicine, Ankara, Turkey (S.D., A.R.A.); and Department of Pharmacology, McGill University, Montreal, QB, Canada (S.N.).

The online-only Data Supplement is available with this article at <http://circ.ahajournals.org/lookup/suppl/doi:10.1161/CIRCULATIONAHA.113.005300/-/DC1>.

Correspondence to Bianca J.J.M. Brundel, PhD, Department of Clinical Pharmacology, University of Groningen, UMCG, A. Deusinglaan 1, 9713AV Groningen, The Netherlands. E-mail B.J.J.M.Brundel@umcg.nl

© 2013 American Heart Association, Inc.

Circulation is available at <http://circ.ahajournals.org>

DOI: 10.1161/CIRCULATIONAHA.113.005300

Table 1. Overview Protective Effects of HDAC Inhibitors in Tachypaced HL-1 Cardiomyocytes and *Drosophila melanogaster*

	Class	HDACs	IC ₅₀	Concentration in HL-1	Concentration in <i>Drosophila</i>	Protection in HL-1	Protection in <i>Drosophila</i>
TSA	I	HDAC1, 2, 3, 8	20 nmol/L HDAC1 ¹⁸	10 nmol/L	1 mmol/L	–	–
	Ila	HDAC4, 5, 7, 9	1.2 nmol/L HDAC6 ¹⁸				
	Ilb	HDAC6, 10					
	IV	HDAC11					
Sodium Butyrate	I	HDAC1, 2, 3, 8	30 μmol/L HDAC1 ¹⁹	2 mmol/L	20 mmol/L	–	–
	Ila	HDAC4, 5, 7, 9					
Nicotinamide	III	Sirt1-Sirt7	88 μmol/L Sirt1 ²⁰	10 mmol/L	100 mmol/L	†	*
Tubacin	Ilb	HDAC6	4 nmol/L HDAC6 ¹⁸	1 μmol/L	10 μmol/L	*	*

HDAC indicates histone deacetylase; TSA, Trichostatin A; and –, no significant protective effect.

**P*<0.01 vs control tachypaced; †*P*<0.001 vs control tachypaced.

proteostasis has been implicated in the pathogenesis of multiple diseases, including cardiovascular disorders.⁵ Importantly, the packaging of chromatin is largely dependent on the acetylation status of histones,⁶ which is controlled by histone acetyltransferases and histone deacetylases (HDACs). Evidence for epigenetic regulation in AF originates from observations that the (re)activation of the fetal gene program in cardiomyocytes promotes AF.^{7,8} Furthermore, genetically modified mice with increased HDAC activity are prone to develop atrial arrhythmia and to reveal substrates for AF such as a reduction in connexin40 expression, cardiac hypertrophy, and fibrosis.⁹ Thus,

Table 2. Baseline Demographic and Clinical Characteristics of Patients With PAF, Patients With PeAF, and Control Patients in Sinus Rhythm

	Sinus Rhythm	PAF	PeAF
n	17	13	28
RAA, n	17	13	25
LAA, n	14	11	27
Age, y	58±5	50±3	61±3
Duration of AF, median (range), mo	–	–	8 (0.1–56)
Time in sinus rhythm before surgery, median (range), d	–	10 (0.5–210)	–
Duration of last episode AF, median (range), h	–	12 (0.2–24)	–
AF, median (range), d	–	2 (0.2–70)	–
Underlying heart disease/surgical procedure, n (%)			
Lone AF/Maze	0 (0)	7 (54)	7 (25)
MV disease/MV replacement or repair	17 (100)	6 (46)	21 (75)
Medication, n (%)			
ACE/ARB	10 (59)	5 (38)*	15 (54)
Digoxin	1 (6)	1 (8)	11 (39)*
Calcium channel blocker	5 (29)	3 (23)	8 (29)
β-Blocker	13 (77)	3 (23)*	8 (29)

Values are presented as mean±SEM when appropriate. Maze is atrial arrhythmia surgery. ACE indicates angiotensin-converting enzyme; AF, atrial fibrillation; ARB, angiotensin receptor blocker; LAA, left atrial appendage; MV, mitral valve; PAF, paroxysmal atrial fibrillation; PeAF, permanent atrial fibrillation; and RAA, right atrial appendage.

**P*<0.05 vs sinus rhythm.

HDACs substantially affect cardiomyocyte proteostasis and may participate in AF progression.

HDACs not only affect the protein acetylation status of histones but also target many cytoplasmic proteins, including structural proteins such as α-tubulin.^{10–12} α-Tubulin is a key component of the microtubule network, and its acetylation influences microtubular composition and organization, thereby modulating Ca²⁺ signaling and contractility.^{13,14} Thus, acetylation of α-tubulin may represent a second mechanism by which HDACs influence cardiomyocyte proteostasis and AF progression.⁵

Recently, progress has made in understanding the crucial role of HDACs in cardiac development and pathogenesis.^{4,15} Eighteen mammalian HDACs are classified into 5 groups based on their structure, complex formation, and expression pattern: class I (HDAC1, 2, 3, and 8), class IIa (HDAC4, 5, 7, and 9), class IIb (HDAC6 and 10), class III (Sirt1–7), and class IV (HDAC11).⁴ Several HDAC inhibitors reveal promising therapeutic effects in that they attenuate cardiac hypertrophy, fibrosis, and contractile dysfunction in mice atria.^{4,9} However, the specific HDACs that contribute to the development of a substrate for AF are still unknown. The aim of the present study was to identify HDACs involved in the structural and functional remodeling in AF with the use of cellular and in vivo experimental models, as well as atrial tissue samples from AF patients.

Methods

This section contains a brief summary of the principal methods. For details, see the online-only Data Supplement.

HL-1 Cardiomyocyte Model

HL-1 cardiomyocytes derived from adult mouse atria were obtained from Dr William Claycomb (Louisiana State University, New Orleans) and cultured as previously described.^{16,17} The cardiomyocytes were normal paced (1 Hz) or tachypaced (5 Hz) with a C-Pace100 culture pacer (IonOptix Corp, Milton, MA). Ca²⁺ transient (CaT) measurements were performed as previously described.^{16,17}

Before pacing, HL-1 cardiomyocytes were treated with the HDAC inhibitors described in Table 1. All inhibitors were obtained from Sigma. The nonactive analog niltubacin (1 μmol/L) was added as a control for tubacin. To study the effect of HDAC6 on CaT, HL-1 cardiomyocytes were transfected with pcDNA3.1+ (empty plasmid), HDAC6 wild type, HDAC6 mutant in the first catalytic domain (HDAC6 m1), HDAC6 mutant in the second catalytic domain

(HDAC6 m2), or HDAC6 mutant in both domains (HDAC6 m1-2) by the use of Lipofectamine 2000 (Invitrogen). The HDAC6 plasmids were a kind gift from Dr Alexander Bershadsky.

Drosophila Stocks, Tachypacing, and Heart Wall Contraction Assays

Wild-type W1118 strains were obtained from Genetic Services Inc. All flies were maintained at 25°C on standard medium. After fertilization, adult flies were removed, and HDAC inhibitors (Table 1) were added to the medium containing fly embryos. After 2 days, prepupae were selected for tachypacing, as previously described.^{21,22} Briefly, transparent pupae were placed on 1% agarose gel in PBS. Groups of 5 pupae were subjected to tachypacing (4 Hz for 20 minutes) by the use of a C-Pace100 culture pacer (IonOptix Corp). Before and after tachypacing, movies of whole pupae visualized through a microscope at $\times 10$ magnification were obtained in triplicate periods of 10 seconds. Heart wall contractions were analyzed with image J software.

Canine Model

Animal handling procedures followed National Institutes of Health guidelines (NIH Publication No. 85-23, revised 1996) and were approved by the Animal Research Ethics Committee of the Montreal Heart Institute. Adult mongrel dogs were divided into 3 groups: sham with administration of tubastatin A vehicle (n=6; mean body weight, 25.2 \pm 1.2 kg), atrial tachypacing with administration of tubastatin A vehicle (ATP; n=6; mean body weight, 25.7 \pm 0.8 kg), and ATP with tubastatin A 1 mg \cdot kg⁻¹ \cdot d⁻¹ administered with continuous infusion via osmotic pump (n=6; mean body weight, 25.7 \pm 1.3 kg). All dogs underwent the same surgical procedure and AF induction measurements, as mentioned in the online-only Data Supplement.

Atrial Cardiomyocyte Isolation

After electrophysiological study, the heart was excised and immersed in oxygen-saturated Tyrode solution (in mmol/L: NaCl 136, KCl 5.4, MgCl₂ 1, CaCl₂ 2, NaH₂PO₄ 0.33, HEPES 5, and dextrose 10, pH 7.35

by NaOH). The left atrium was isolated from the heart with intact blood supply and used to isolate cardiomyocytes as described in the online-only Data Supplement.

Ca²⁺ Imaging and Cellular Contractility Assessment

Atrial cardiomyocytes were incubated with indo-1 AM (5 μ mol/L, dissolved in pluronic F-127 2.5 μ g/mL in 20% dimethyl sulfoxide) for 8 minutes followed by perfusion with Tyrode solution containing 1.8 mmol/L Ca²⁺ for 40 minutes before measurement. An integrated system (IonOptix Corp) with a video-based edge-detection device and dual-excitation fluorescence photomultiplier was used to monitor Ca²⁺ transients and cell contractility. Further experimental details are given in the online-only Data Supplement.

Cell Electrophysiology Recordings

The whole-cell perforated-patch technique was used to record action potentials at 37°C and 1 Hz in current-clamp mode and tight-seal patch clamp to record currents in voltage-clamp mode at 37°C as described in the online-only Data Supplement. Clampfit 9.2 (Axon), GraphPad Prism 5.0, and Origin 5.0 were used for data analysis.

Patients

Before surgery, 1 investigator assessed patient characteristics (Table 2), as described before.¹⁷ Right and left atrial appendages were obtained from patients with paroxysmal fibrillation (PAF) and permanent AF (PeAF) and control patients in sinus rhythm. The PeAF and PAF group included patients with lone AF or AF with underlying mitral valve disease. After excision, atrial appendages were immediately snap-frozen in liquid nitrogen and stored at -80°C. The study conforms to the principles of the Declaration of Helsinki. The Institutional Review Board approved the study, and patients gave written informed consent. Tissue was used to perform various assays. Unfortunately, the tissue yield per patient was insufficient for all assays to be performed on each patient sample. However, at least 3 samples per group were used for the individual tests, as indicated in the figure legends.

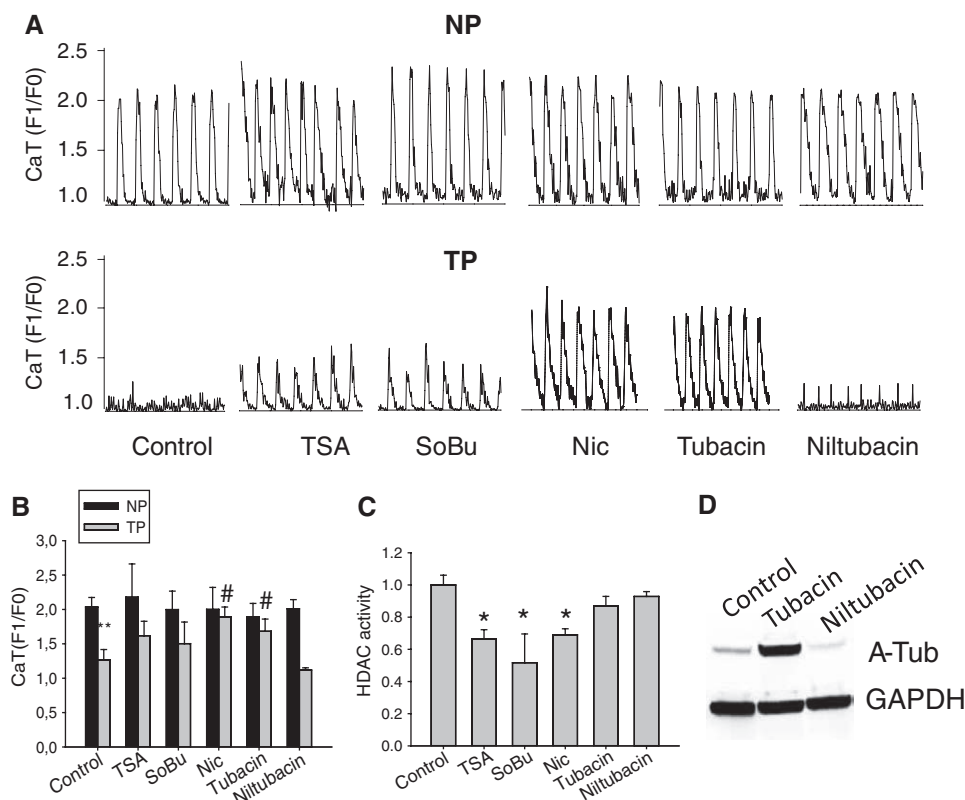


Figure 1. Histone deacetylase-6 (HDAC6) and sirtuin inhibitors protect against Ca²⁺ transient (CaT) reductions in tachypaced (TP) HL-1 cardiomyocytes.

A, Representative CaT of HL-1 cardiomyocytes after normal pacing (NP; 1 Hz) or TP (5 Hz). HL-1 cardiomyocytes were pretreated with TSA, sodium butyrate (SoBu), nicotinamide (Nic), tubacin, or niltubacin, followed by NP or TP and measurement of CaT. **B**, Quantified CaT amplitude of NP and TP HL-1 cardiomyocytes, each from the groups indicated. ** $P < 0.01$ vs control NP; # $P < 0.05$ vs control TP; $n \geq 15$ cardiomyocytes for each group. **C**, The efficiency of pan-HDAC inhibitors was tested by use of an HDAC activity assay, and **(D)** the activity of the specific HDAC6 inhibitor tubacin was tested by Western blot analysis of acetylated α -tubulin (A-Tub). The concentration of drugs used is given in Table 1. * $P < 0.05$ vs control. TSA indicates Trichostatin A.

Calpain Activity Measurement

The calpain activity measurement in human tissue was performed as described previously.¹⁷ Suc-Leu-Leu-Val-Tyr-7-amino-4-methylcoumarin (AMC; Sigma), was used as calpain substrate. Protein extracts (25 µg) were added to 20 µmol/L AMC in 300 µL Tris-buffered saline. AMC release was measured by fluorometry (360-nm excitation, 430-nm emission; Spectrometer LS50B, PerkinElmer) after 30 minutes of incubation at room temperature.

HDAC and HDAC6 α-Tubulin Deacetylase Activity Domain Activity Measurements

The overall HDAC activity was measured by use of a fluorometric HDAC activity assay kit (Sigma) according to the manufacturer’s instructions (for details, see the online-only Data Supplement). The HDAC6 activity assay was developed as previously described with minor changes.²³ Atrial tissue samples were lysed in nondenaturing buffer (CellLytic, Sigma) supplemented with protein inhibitor cocktail (Roche). HL-1 cardiomyocytes and cardiomyocytes isolated from dogs were lysed in PBS (pH 7.4) containing 0.5% Triton X-100 and protein inhibitor cocktail (Roche), followed by sonification and

centrifugation. Protein concentrations were determined by Bio-Rad Protein Assay Kit (Biorad), and 30 µg of HL-1 cardiomyocytes, 50 µg of dog cardiomyocytes, or 100 µg of human tissue extracts was diluted in PBS buffer (total volume, 100 µL) in a 96-well plate. The HDAC6 inhibitor tubacin (30 µmol/L), which inhibits the α-tubulin deacetylase activity (TDAC) domain of HDAC6, or vehicle was added (30 minutes at 37°C). Then, 5 µL of 1 mmol/L stock solution of synthetic HDAC class I/IIb substrate I-1875 (Bachem) was added (2.5 hours at 37°C). The reaction was stopped with 50 µL of stop solution (PBS with 1.5% Triton X-100, 3 µmol/L Trichostatin A (TSA), and 0.75 mg/mL trypsin). Fluorescence was measured by a BioTek Synergy 4 plate reader (360-nm excitation, 460-nm emission). Background signals were subtracted. To correct for quenching of the AMC signal by colored tissue extracts, an additional reference set of samples and buffer blanks with AMC (Alfa Aesar, 5 µL of 80-µmol/L stock) instead of substrate was included. The reference AMC signals were used to calculate quenching ratios relative to the AMC buffer blank signal. Each raw fluorescence value from the substrate-containing samples was divided by the corresponding quenching ratio, followed by subtraction of the substrate background. HDAC6 TDAC domain activity was calculated as the amount of HDAC activity blocked by tubacin.

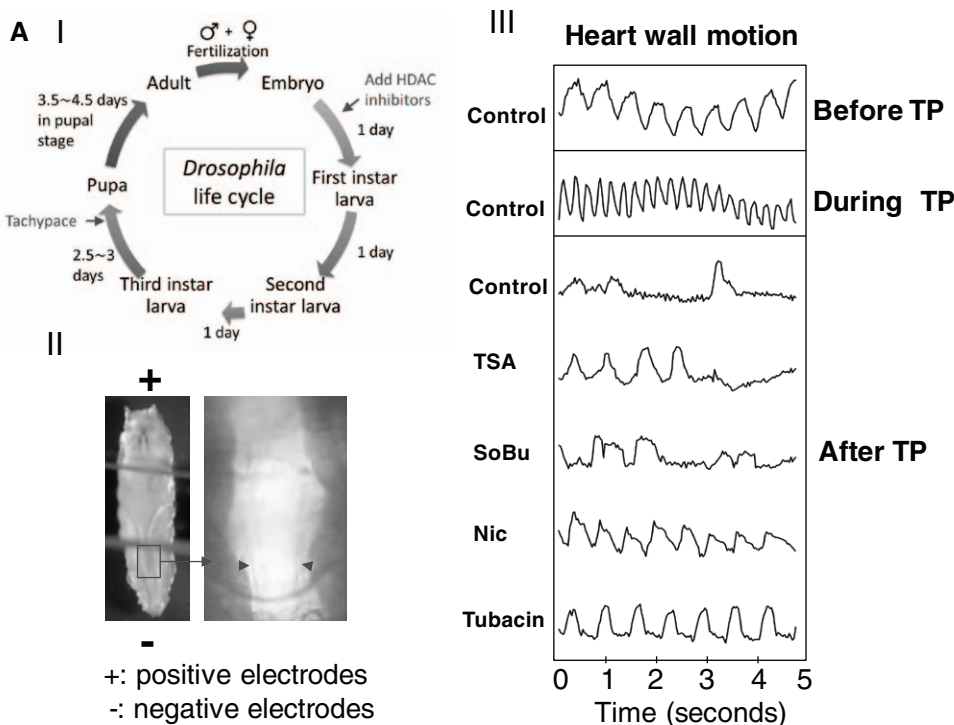
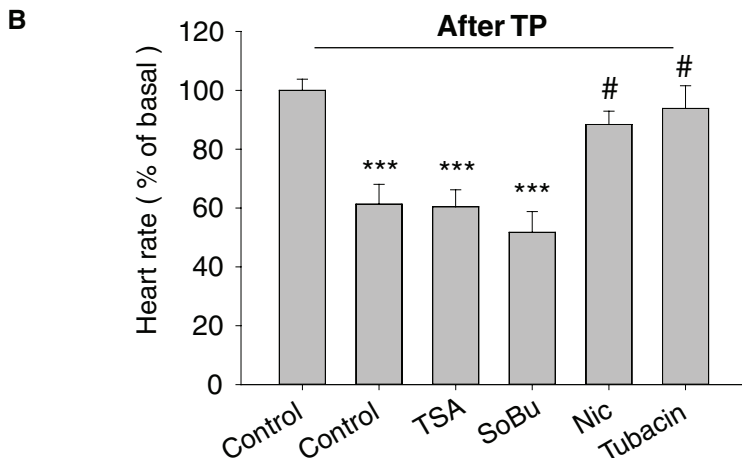


Figure 2. Histone deacetylase-6 (HDAC6) and sirtuin inhibitors protect against tachypacing (TP)-induced contractile dysfunction in the heart wall of *Drosophila melanogaster*. **A, I**, HDAC inhibitors were added to the food, and prepupae were selected for normal (NP) or TP (arrows). **II**, Prepupae were subjected to TP by placing them on an agarose gel connected to electrodes, followed by monitoring of the heart wall contraction rate. **III**, Representative heart wall contractions monitored before, during, and after TP with or without pretreatment with Trichostatin A (TSA), sodium butyrate (SoBu), nicotinamide (Nic), or tubacin at the concentrations indicated in Table 1. **B**, Quantified data showing heart wall contraction rates each from groups as indicated. ****P*<0.001 vs control before TP; #*P*<0.01 vs control TP; n=9 to 18 pupae for each group.



Protein Extraction and Western Blot Analysis

HL-1 or dog cardiomyocytes or tissue samples were lysed in radioimmunoprecipitation assay buffer as described before.¹⁷ In short, equal amounts of protein were separated on SDS-PAGE gels, transferred onto nitrocellulose membranes, and probed with anti-acetylated α -tubulin (Sigma), anti- α -tubulin (Sigma), anti-human HDAC6 (Cell Signaling), anti-mouse HDAC6 (Cell Signaling), anti-HA tag (Sigma), or anti-GAPDH (Fitzgerald). Blots were subsequently incubated with horseradish peroxidase-conjugated anti-mouse or anti-rabbit secondary antibodies (Dako). Signals were detected by the ECL detection method (Amersham) and quantified by densitometry (Syngene, Genetools).

Polymerized and Depolymerized α -Tubulin Fractions and Drug Treatment

Polymerized and depolymerized (soluble monomers) α -tubulin was fractionized as previously described with minor changes.²⁴ In brief, after 1 rinse in PBS, HL-1 cardiomyocytes were washed in microtubule-stabilizing buffer (0.1 mol/L PIPES, pH 6.93, 1 mmol/L EGTA, 1 mmol/L MgCl₂, 2 mol/L glycerol) and then incubated for 3 minutes with 0.5 mL microtubule-stabilizing buffer containing 0.5% Triton X-100 and protein inhibitor cocktail (Roche). After incubation, the supernatant contained the soluble depolymerized α -tubulin fraction and was transferred to a new tube. The remaining HL-1 cardiomyocytes were washed once with microtubule-stabilizing buffer and then lysed with radioimmunoprecipitation assay buffer. The collected lysate contains the polymerized tubulin.

For testing the effect of drugs on (de)polymerization status of α -tubulin, 20 μ mol/L of the calpain inhibitor PD150606 (Calbiochem) was added to HL-1 cardiomyocytes 2 hours before tachypacing as described before.¹⁷ The HDAC6 inhibitor tubacin (1 μ mol/L) was added to cells 12 hours before tachypacing. HL-1 cardiomyocytes were tachypaced for 8 hours followed by isolation of polymerized and depolymerized α -tubulin fractions as described above.

Statistical Analysis

Results are expressed as mean \pm SEM. Biochemical analyses were performed at least in duplicate. Multiple-group comparisons were obtained by ANOVA, with 1-way ANOVA for nonrepeated measurements and 2-way ANOVA for repeated-measurement analyses. Individual group mean differences were evaluated with the Student *t* test and Bonferroni correction. Correlation was determined with the Spearman correlation test. All *P* values were 2 sided. Values of *P*<0.05 were considered statistically significant. SPSS version 20 was used for all statistical evaluations.

Results

HDAC6 and Sirtuins Mediate Tachypacing-Induced Contractile Dysfunction in Cardiomyocytes and *Drosophila*

We initially determined which HDAC classes were involved in cardiomyocyte remodeling by using various HDAC inhibitors

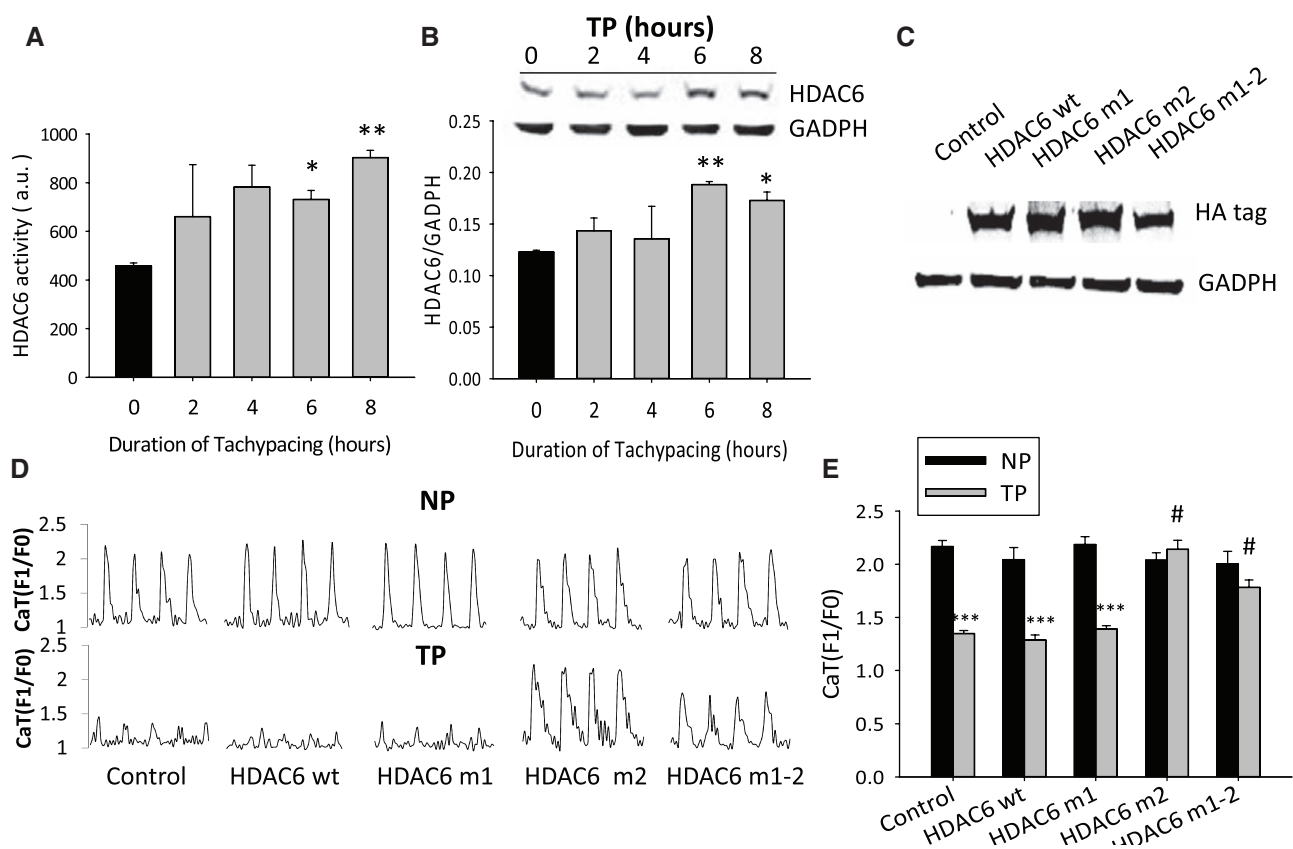


Figure 3. Tachypacing (TP) activates histone deacetylase-6 (HDAC6), and inhibition of tubulin deacetylase activity (TDAC) catalytic domain of HDAC6 rescues TP-induced Ca²⁺ transient (CaT) loss in HL-1 cardiomyocytes. **A**, Time course of TP-induced HDAC6 activity. HDAC6 TDAC activity is significantly increased after 6 and 8 hours of TP. **B**, Western blot showing TP increases the HDAC6 expression level after 6 and 8 hours of TP. **P*<0.05; ***P*<0.01 vs control at 0 hours. **C**, Representative Western blot showing transfected HL-1 cardiomyocytes overexpressing the wild-type HDAC6 (HDAC6 wt) and the 3 mutants with impaired deacetylating activity: HDAC6 m1, HDAC6 m2, and HDAC6 m1-2. Control cells are transfected with empty plasmid, pCDNA3.1. **D**, Representative CaT of normal paced (NP) or TP HL-1 cardiomyocytes transfected with HDAC6 wt, HDAC6 m1, HDAC6 m2, or HDAC6 m1-2. **E**, Quantitative data showing HL-1 cardiomyocytes transfected with HDAC6 m2 or HDAC6 m1-2 reveal protective effects against TP-induced CaT reductions. ****P*<0.001 vs control NP; #*P*<0.001 vs control TP; n=32 to 80 cardiomyocytes for each group.

in tachypaced HL-1 cardiomyocytes and *Drosophila* (Table 1). Inhibition of HDAC6 by tubacin and of sirtuins by nicotinamide protected against the tachypacing-induced reduction of CaT (Figure 1A and 1B and Movies I–VII in the online-only Data Supplement). In contrast, niltubacin (the inactive analog of tubacin) and the pan-HDAC inhibitors TSA and sodium butyrate did not protect against CaT loss, despite reducing overall HDAC activity (Figure 1C and 1D). These findings indicate that HDAC6 and sirtuins are involved in tachypacing-induced remodeling in the in vitro HL-1 cardiomyocyte model. To extend these findings to a second experimental model, similar experiments were conducted in tachypaced *Drosophila*.²² Tachypacing induced a marked reduction in contractility in nontreated *Drosophila* (Figure 2A and 2B). Similar to the findings in tachypaced HL-1 cardiomyocytes, inhibition of HDAC6 and sirtuins attenuated tachypacing-induced contractile dysfunction in *Drosophila*, whereas TSA and sodium butyrate were ineffective (Figure 2A and 2B; see also Figure I and Movies VIII–XVIII in the online-only Data Supplement). Tachypacing did not affect overall HDAC activity significantly in HL-1 cardiomyocytes or *Drosophila* (Figure IIA and IIB in the online-only Data Supplement), indicating activation of specific HDACs during tachypacing.

TDAC of HDAC6 Modulates the Loss of CaT and Microtubule Network Through Deacetylation of α -Tubulin

Because tubacin inhibits HDAC6 by blocking the TDAC domain of HDAC6¹¹ and protects against tachypacing-induced contractile dysfunction in both tachypaced HL-1 cardiomyocytes and

Drosophila, we investigated whether HDAC6 becomes activated by tachypacing. A significant increase in HDAC6 TDAC domain activity and HDAC6 expression (Figure 3A and 3B) was observed after 6 and 8 hours of tachypacing HL-1 cardiomyocytes. To further support HDAC6 involvement, dominant-negative HDAC6 mutants with disrupted catalytic domains were studied. Successful transfection of the various constructs was assessed by Western blot (Figure 3C). HL-1 cardiomyocytes transfected with the control plasmid, wild-type HDAC6, or disruption of the first catalytic domain of HDAC6 (HDAC domain) continued to show significant reductions in CaT after tachypacing (Figure 3D and 3E). In contrast, disruption of the second catalytic domain (TDAC domain) of HDAC6 or both HDAC and TDAC domains rescued tachypaced HL-1 cardiomyocytes from CaT loss (Figure 3D and 3E). This finding demonstrates that tachypacing-induced CaT reduction is mediated by the TDAC activity of HDAC6.

Because the TDAC domain of HDAC6 conveys the deacetylation of α -tubulin,¹¹ the expression of acetyl α -tubulin over the time course of tachypacing was determined. Tachypacing caused a significant reduction in α -tubulin acetylation after 6 hours (Figure 4A and 4B), which was followed by a significant reduction in total α -tubulin levels after 8 hours (Figure 4A and 4C). Tubacin attenuated both the tachypacing-induced deacetylation and degradation of α -tubulin (Figure 4D–4F). The reduction in acetyl α -tubulin was specific because no significant changes in the overall acetylation level of proteins or histones were observed between control and tachypaced HL-1 cardiomyocytes (Figure III in the online-only Data Supplement).

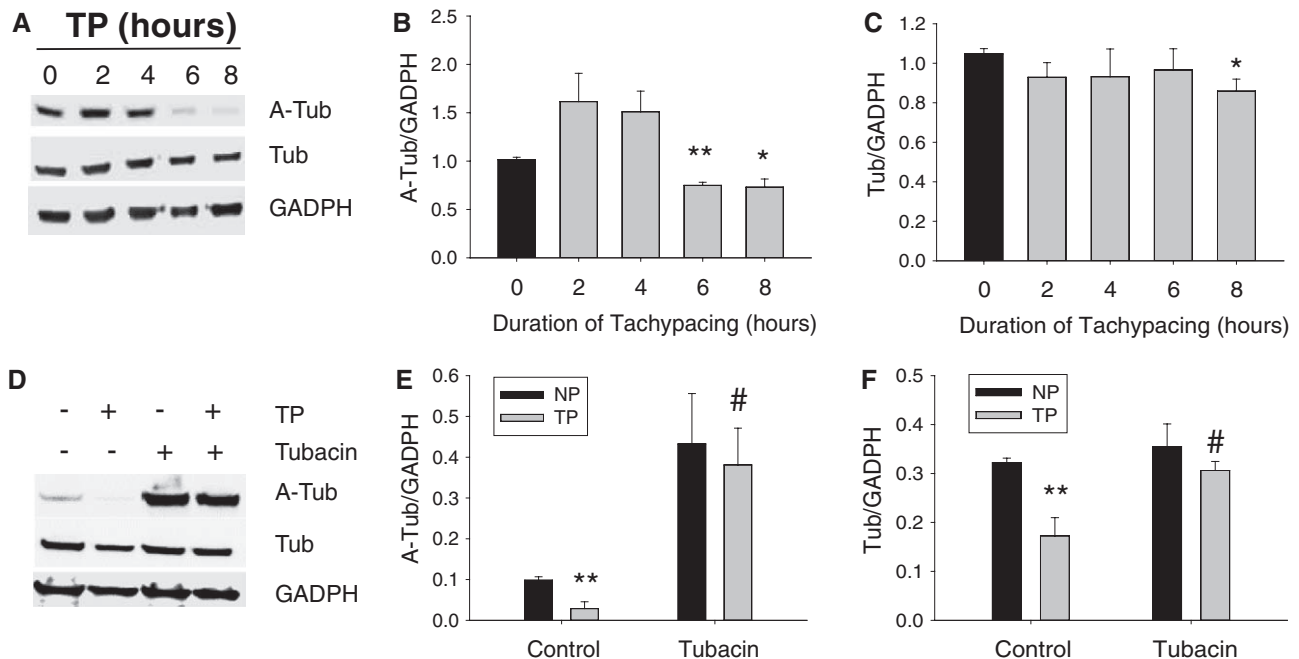


Figure 4. Tachypacing (TP) induces deacetylation and degradation of α -tubulin (Tub), which is prevented by histone deacetylase-6 (HDAC6) inhibition. **A**, Representative Western blot showing TP-induced reductions in acetyl α -tubulin (A-Tub) and degradation of α -tubulin. **B** and **C**, Quantified data of 3 independent Western blots showing a significant reduction in acetyl α -tubulin after 6 hours and α -tubulin after 8 hours of tachypacing. * $P < 0.05$; ** $P < 0.01$ vs control at 0 hours of TP. **D**, Representative Western blot showing HDAC6 inhibition by tubacin protects against tachypacing-induced deacetylation and degradation of α -tubulin. **E** and **F**, Quantified data of 3 independent Western blots showing the amount of acetyl α -tubulin (**E**) and α -tubulin (**F**) for the treatments as indicated. Control HL-1 cardiomyocytes were treated with dimethyl sulfoxide (solvent of tubacin). ** $P < 0.01$ vs control normal pacing (NP); # $P < 0.01$ vs control TP.

α -Tubulin and β -tubulin form the microtubule network, which is made up of structural polymers supporting the architecture, contractile function, and active transport of cytoplasmic constituents, including mitochondria and endoplasmic reticulum.^{5,25} Moreover, HDAC6-induced deacetylation of α -tubulin results in the depolymerization of microtubules^{12,26,27} and thereby impairs CaT.¹⁴ To examine whether tachypacing-induced HDAC6 activation causes CaT loss via depolymerization of microtubules, HL-1 cardiomyocytes were stained for α -tubulin and acetyl α -tubulin, and the structure of microtubules was determined in cardiomyocytes treated with or without tubacin. Tachypacing significantly reduced the amount of total α -tubulin and acetyl α -tubulin, an effect prevented by tubacin (Figure 5A and 5B). In addition, tachypacing significantly reduced the amount of polymerized microtubules, indicating disruption of the microtubule structure (Figure 5A and 5B). Finally, tubacin protected against tachypacing-induced depolymerization of microtubules (Figure 5A and 5B). The polymerization of α -tubulin was assessed by separation of polymerized from depolymerized microtubules in control and tachypaced HL-1 cardiomyocytes. Similar to confocal experiments, tubacin

attenuated the tachypacing-induced reduction of polymerized and depolymerized α -tubulin (Figure 5C). These observations demonstrate that tachypacing induces deacetylation and depolymerization of α -tubulin and subsequent disruption of the microtubules. Although acetylated α -tubulin is a substrate for both HDAC6 and Sirt2, the sirtuin inhibitor nicotinamide did not prevent tachypacing-induced deacetylation, depolymerization, and degradation of α -tubulin (Figure IV in the online-only Data Supplement). Overall, these findings indicate a prominent role for HDAC6 in tachypacing-induced cardiomyocyte remodeling through TDAC-induced deacetylation and depolymerization of α -tubulin and subsequent disruption of the microtubule network and loss of CaT.

Tachypacing Induces Calpain-Mediated Degradation of Depolymerized α -Tubulin

The Ca^{2+} -dependent protease calpain is known to degrade depolymerized but not polymerized α -tubulin.²⁸ Because we previously demonstrated a key role for activated calpain in the degradation of contractile proteins in experimental and human AF,^{20,29} we tested its involvement in the tachypacing-induced degradation of depolymerized α -tubulin. Inhibition

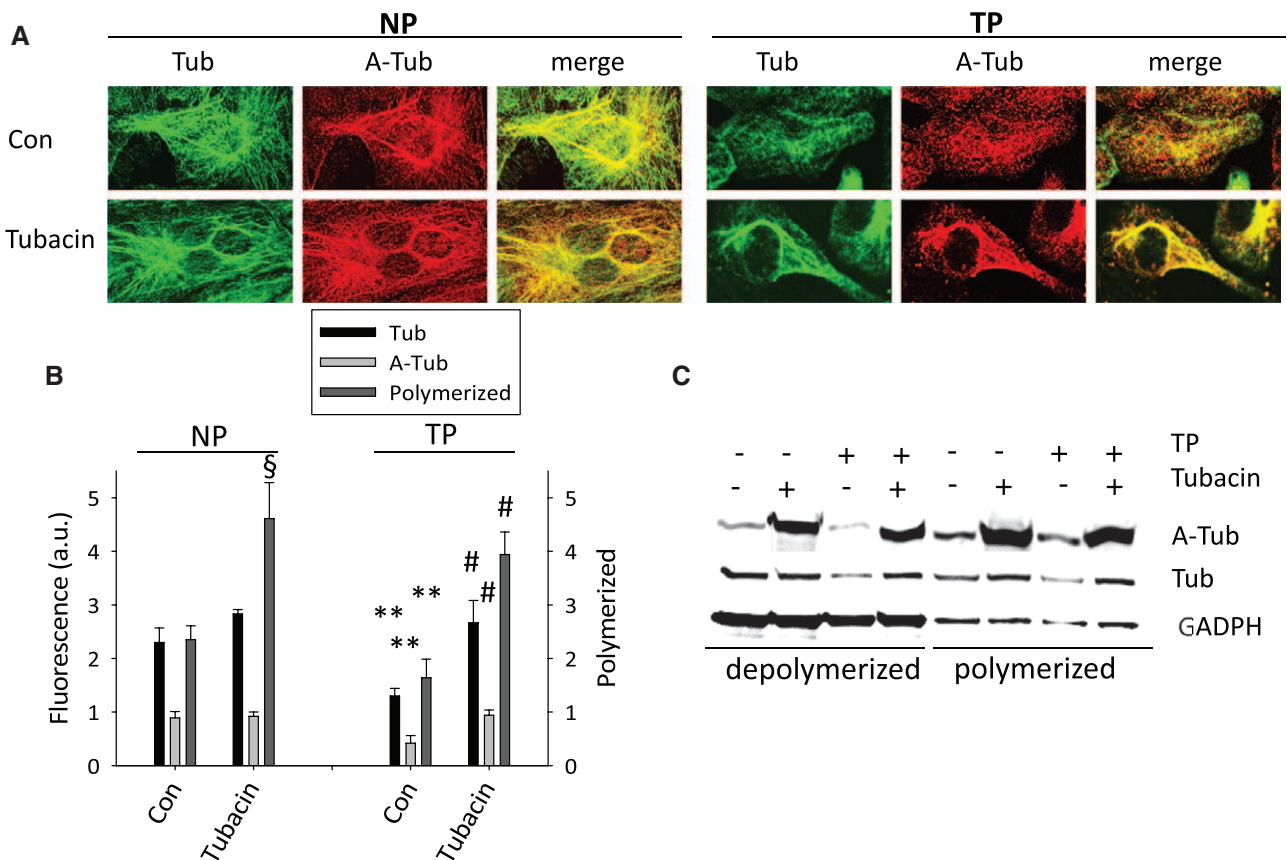


Figure 5. Inhibition of histone deacetylase-6 (HDAC6) protects against tachypacing (TP)-induced degradation of α -tubulin (Tub) and depolymerization of microtubules. **A**, Typical example of an immunofluorescent staining of α -tubulin (green) and acetyl α -tubulin (A-Tub; red) in normal paced (NP) and TP HL-1 cardiomyocytes. TP induces depolymerization of microtubules (yellow), which is preserved by tubacin. **B**, Quantification of the amount of acetyl α -tubulin, α -tubulin, and polymerized microtubules in NP and TP HL-1 cardiomyocytes. TP significantly decreased the amount of acetyl α -tubulin, α -tubulin, and polymerized α -tubulin, which was prevented by tubacin. Number of cardiomyocytes per condition: 100 to 250. **C**, Representative Western blot showing TP-induced reductions in polymerized α -tubulin and degradation of depolymerized α -tubulin, in line with decreased acetylation of polymerized and depolymerized α -tubulin (A-Tub). Tubacin protected against the depolymerization and degradation of α -tubulin and revealed increased levels of acetyl α -tubulin. GAPDH was used to show successful separation of polymerized and depolymerized fractions. Control HL-1 cardiomyocytes were treated with dimethyl sulfoxide (solvent of tubacin). ** $P < 0.01$ vs control NP; # $P < 0.01$ vs control TP; § $P < 0.01$ vs control NP.

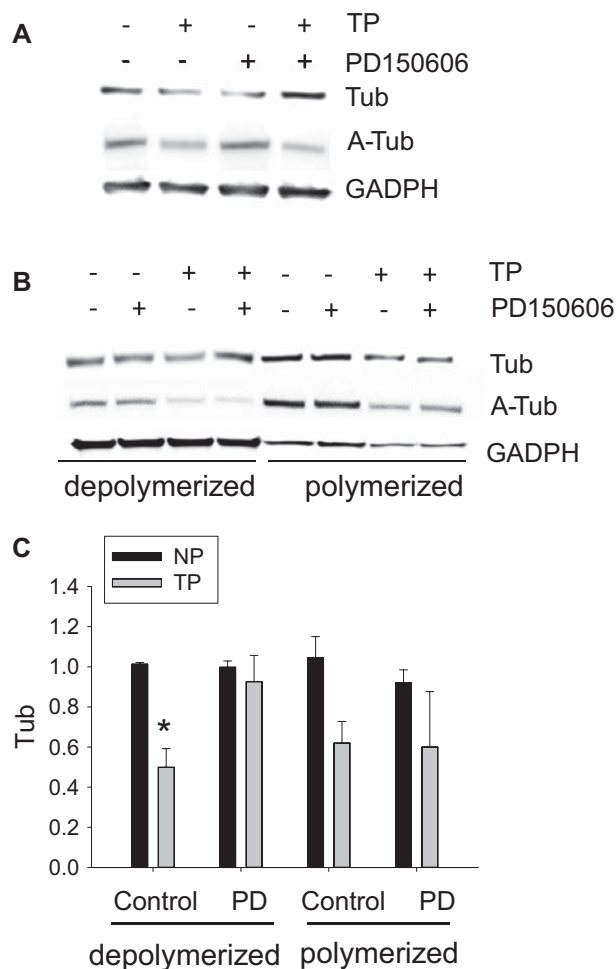


Figure 6. Calpain inhibitor PD150606 attenuates tachypacing (TP)-induced degradation of depolymerized α -tubulin (Tub). **A**, Representative Western blot showing that pretreatment with calpain inhibitor PD150606 attenuates TP-induced α -tubulin degradation. **B**, Representative Western blot showing the effect of PD150606 on TP-induced reductions in polymerized α -tubulin and degradation of depolymerized α -tubulin. TP-induced degradation of depolymerized α -tubulin is attenuated by PD150606 (PD). No effect of PD150606 on the amount of TP-induced depolymerization (Tub) or deacetylation of α -tubulin (A-Tub) was observed. GADPH was used to indicate the successful separation of polymerized and soluble α -tubulin. **C**, Quantification of 3 independent experiments showing TP-induced degradation of depolymerized α -tubulin, which was prevented by PD150606. * $P < 0.05$ vs control normal pacing (NP).

of calpain by PD150606 mitigated tachypacing-induced degradation of α -tubulin (Figure 6A). Furthermore, PD150606 only attenuated the degradation of depolymerized α -tubulin without affecting the depolymerization status of microtubules or deacetylation of α -tubulin (Figure 6B and 6C and Figure V in the online-only Data Supplement). Together, these data imply that deacetylated and depolymerized microtubules are susceptible to degradation by calpain.

Increased HDAC6 Activity Modulates Calpain-Induced Degradation of α -Tubulin in Patients With AF

To investigate whether similar changes in HDAC6 are found in patients with AF, HDAC6 TDAC domain activity and

HDAC6 expression were determined in the left and right atrial appendages of PeAF patients and control subjects in sinus rhythm. Both HDAC6 TDAC domain activity and HDAC6 expression were significantly increased in patients with PeAF compared with those in sinus rhythm (Figure 7E and 7F), and HDAC6 activity correlated with the duration of PeAF (Figure VID in the online-only Data Supplement). Furthermore, the amount of acetylated α -tubulin and total tubulin was determined in control subjects in sinus rhythm and patients with PAF or PeAF. PAF and PeAF patients showed a significant reduction in the amount of acetylated α -tubulin (Figure 7A and 7B). Reduction of acetylated α -tubulin was more pronounced in left versus right atrial appendages in patients with PeAF and inversely correlated with the duration of AF (Figure VIA, VIB, VIE, and VIF in the online-only Data Supplement). Furthermore, similar to the findings in experimental models, both the total HDAC activity and overall acetylation level of proteins did not differ between patients with PeAF, patients with PAF, and control subjects in sinus rhythm (Figure IIC and IIIC in the online-only Data Supplement). Total α -tubulin levels were significantly reduced in PAF and PeAF patients (Figure 7A and 7C), and α -tubulin levels correlated inversely with calpain activity in left atrial appendage (Figure 7D and Figure VIC in the online-only Data Supplement). Thus, the results in human AF are in line with the experimental findings in tachypaced HL-1 cardiomyocytes.

HDAC6 Inhibition by Tubastatin A Protects Against AF-Related Remodeling in Dogs

To obtain proof of concept that HDAC6 inhibition protects against AF remodeling in vivo, dogs subjected to 7 days of ATP were treated with the HDAC6 inhibitor tubastatin A (1 mg·kg⁻¹·d⁻¹). ATP substantially increased the duration of AF in untreated animals, an effect prevented by tubastatin A (Figure 8A). Furthermore, tubastatin A protected against ATP-induced electrical remodeling (action potential duration shortening, I_{CaL} reduction; Figure 8B and 8C), as well as CaT reduction and contractile dysfunction (loss of cell shortening and sarcomere contractility; Figure 8D–8F). Finally, HDAC6 activity and HDAC6 expression were significantly increased in ATP dogs (Figure 8G and 8H), and tubastatin A attenuated the ATP-induced HDAC6 TDAC domain activity enhancement in ATP dogs (Figure 8G). Although degradation of α -tubulin was not observed in ATP dogs, the ratio of acetylated α -tubulin to total α -tubulin was reduced in ATP dogs and was not significantly changed by ATP in tubastatin A–treated dogs (Figure 8I). Thus, HDAC6 appears to play a significant role in AF-related remodeling in vivo.

Discussion

Here, we identify HDAC6 as a potentially key enzyme in the development of the substrate underlying AF progression. Tachypacing of HL-1 cardiomyocytes increases HDAC6 activity and expression, resulting in TDAC domain–dependent deacetylation/depolymerization and calpain-mediated degradation of α -tubulin with subsequent disruption of the microtubule network. HDAC6 inhibition by tubastatin conserved the microtubule structure and prevented

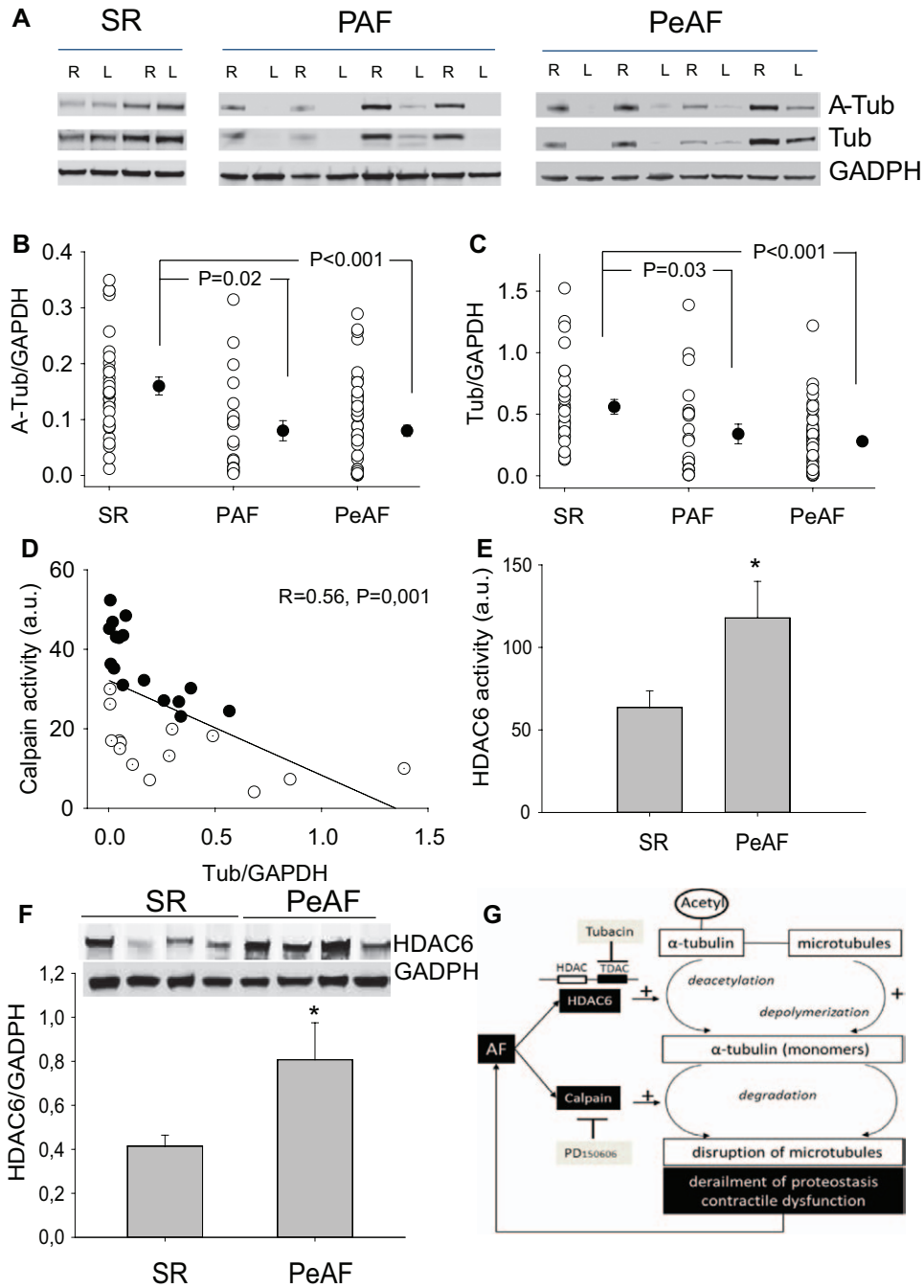


Figure 7. Patients with atrial fibrillation AF reveal reduced levels of acetylated (A-Tub) and total α -tubulin (Tub) and induction of histone deacetylase-6 (HDAC6) activity and expression. **A**, Representative Western blot of α -tubulin and acetyl α -tubulin and GADPH in patients with paroxysmal AF (PAF), permanent AF (PeAF), and control sinus rhythm (SR). **B**, Quantification of acetyl α -tubulin and **(C)** α -tubulin in patients with SR, PAF, and PeAF showing a significant reduction in α -tubulin and acetyl α -tubulin in PAF and PeAF compared with SR. **D**, Significant inverse correlation between tissue calpain activity and the amount of α -tubulin in the left atrial appendage. ● Indicates PAF (n=11); (○), PeAF (n=16); and ○, SR (n=3). **E**, HDAC6 tubulin deacetylase activity (TDAC) activity is induced in PeAF (n=15) compared with SR (n=18). **P*<0.05 vs SR. **F**, **Top**, Representative Western blot of HDAC6 and GADPH expression levels in patients with PeAF and control subjects in SR. **Bottom**, Quantified data showing a significant increase in HDAC6 expression in PeAF compared with SR (n=23 for SR, n=21 for PeAF). **G**, Proposed model for AF-induced HDAC6 activity as a key enzyme in the derailment of α -tubulin proteostasis, microtubule disruption, and contractile dysfunction, which underlie AF progression. HDAC6 causes α -tubulin deacetylation and subsequent depolymerization of microtubules into monomeric α -tubulin, which are degraded by calpain. Tubacin blocks TDAC activity of HDAC6 and thereby prevents the initial α -tubulin deacetylation and further downstream effects of derailment. PD150606 blocks the activation of calpain, thereby preventing degradation of α -tubulin but not AF-induced deacetylation and depolymerization of microtubules.

depolymerized α -tubulin from degradation by calpain. Ultimately, this derailment of α -tubulin proteostasis causes contractile dysfunction (proposed model in Figure 7G).

Consistent with our experimental data, patients with PeAF show increased HDAC6 TDAC domain activity and expression, as well as increased deacetylation and degradation of

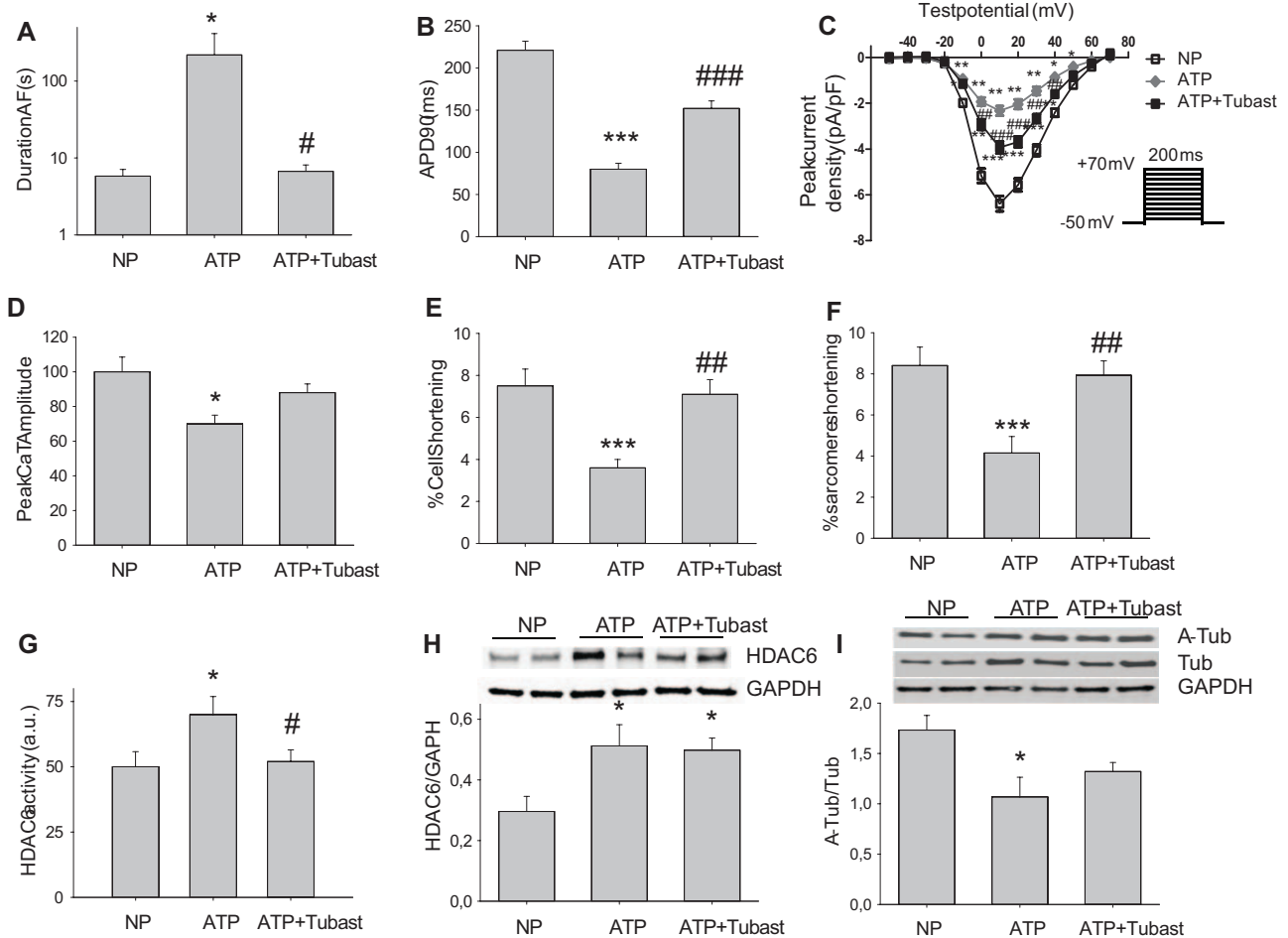


Figure 8. The histone deacetylase-6 (HDAC6) inhibitor tubastatin A protects against atrial remodeling in a dog model for atrial fibrillation (AF). ATP-induced atrial remodeling measured as (A) the duration of induced AF (n=6 dogs for all groups), (B) shortening of action potential duration (APD90; n=15–29 cardiomyocytes), (C) reductions in L-type Ca^{2+} current (I_{CaL} ; n=21–27 cardiomyocytes), (D) loss of Ca^{2+} transient (n=19–38 cardiomyocytes), (E) loss of cell shortening (n=13–31 cardiomyocytes), and (F) loss of sarcomere shortening (n=19–55 cardiomyocytes). All ATP-induced atrial remodeling end points were significantly attenuated by tubastatin A treatment. G, HDAC6 tubulin deacetylase activity (TDAC) activity is induced in ATP and attenuated in ATP dogs treated with tubastatin A. H, Top, Representative Western blot. Bottom, Quantified data revealing HDAC6 expression to be induced in ATP only and ATP tubastatin A dogs. I, Top, Representative Western blot of α -tubulin (Tub) and acetyl α -tubulin (A-Tub) and GAPDH in groups as indicated. Bottom, Ratio of acetyl α -tubulin to α -tubulin is reduced in ATP dogs and attenuated in ATP dogs treated with tubastatin A. * P <0.05, ** P <0.01, *** P <0.001 vs nonpaced (NP) dogs; # P <0.05, ## P <0.01, ### P <0.001 vs ATP dogs.

α -tubulin, which inversely correlates with calpain activity. Finally, in vivo HDAC6 inhibition by tubastatin A protected against atrial remodeling in a dog model of AF. Together, our results identify inhibition of the TDAC domain of HDAC6 as a promising upstream therapeutic target to conserve α -tubulin proteostasis and to attenuate cardiomyocyte remodeling in AF.

Prominent Role for HDAC6 in AF-Induced Loss of Proteostatic Control

The present study identifies HDAC6 as the most prominent HDAC in AF and a key enzyme in the derailment of the proteostasis that underlies structural and functional remodeling and AF progression.³ HDAC6, a member of the class IIb HDACs, is essentially cytoplasmic.³⁰ HDAC6 deacetylates α -tubulin,¹⁰ which impairs control of cell proteostasis by depolymerization of the microtubule network.^{12,26,27} This function of HDAC6 is involved not only in protein misfolding

diseases such as Parkinson disease³¹ and Huntington disease³² but also in cancer.³³ Furthermore, HDAC6 is the only cytosolic HDAC with 2 catalytic domains.³⁴ The second domain is responsible mainly for its TDAC activity.^{4,35} Several lines of evidence suggest that HDAC6 promotes AF by deacetylation of α -tubulin. First, tachypacing-induced remodeling was prevented by treatment with the specific HDAC6 inhibitor tubacin, a drug mainly inhibiting the TDAC domain of HDAC6.¹¹ In accordance with this, we found that tubacin exclusively changed acetylation status of α -tubulin with no effect on overall protein or histone acetylation. Others have also shown that HDAC6 inhibition by tubacin increases the acetylation of α -tubulin.²⁶ Second, dominant-negative mutation of the TDAC domain of HDAC6, the domain conveying the deacetylation of α -tubulin, prevented tachypacing-induced reduction of CaT, whereas dominant-negative mutation of its histone acetylating domain was without protective effect. In accordance

with these findings in experimental AF, we found increased TDAC activity of HDAC6 in patients with PeAF to coincide with deacetylation of α -tubulin.

In addition, we identified depolymerization of the microtubule network as the likely downstream step conveying the action of tachypacing-induced HDAC6 activation underlying AF progression. Our results demonstrate HDAC6-induced deacetylation of α -tubulin to promote a shift from the polymerized microtubule structure toward the depolymerized form, which is susceptible to degradation by the protease calpain. Accordingly, in patients with PeAF, we found both activation of HDAC6 and deacetylation and degradation of α -tubulin, which correlated inversely with calpain activity. These results indicate disruption of the microtubule structure in patients with PeAF. Disrupted microtubule structure causes reductions in contraction,³⁵ I_{CaL} ,³⁶ connexin40 levels⁹ and CaT amplitude³⁷ in cardiomyocytes and therefore might also underlie AF progression.³ The involvement of calpain is in accord with our previous observations that calpain is strongly activated during experimental and clinical AF^{17,22,29} and with data showing degradation of brain α -tubulin by calpain.²⁸

In addition to tubacin, the sirtuin inhibitor nicotinamide protected cardiomyocytes and *Drosophila* from tachypacing. It is conceivable that inhibition of deacetylation of α -tubulin also underlies the protective effect of nicotinamide because tubacin and nicotinamide inhibit different HDACs that function in concert.³⁸ However, in contrast to previous reports,³⁸ nicotinamide did not prevent deacetylation and depolymerization of α -tubulin. Other mechanisms may convey a protective effect of nicotinamide in AF such as increased availability of NAD⁺.³⁹ It is unclear which members of the sirtuin family mediate the protective effects of nicotinamide.⁴⁰ Further research is warranted to elucidate the molecular mechanisms of nicotinamide-mediated cardioprotection. Although effective in a model of cardiac hypertrophy,⁹ the pan-HDAC inhibitors sodium butyrate and TSA proved ineffective in our models despite their inhibition of deacetylation of α -tubulin. Most likely, this beneficial effect of pan-HDAC inhibition in our AF models is offset by effects to increase acetylation of other proteins⁴¹ such as histone H4 (Figure VII in the online-only Data Supplement).

Therapeutic Implications

The efficacy of drugs currently used in AF is limited.¹ Thus, pharmacological approaches preventing or limiting the substrate for the promotion of AF (upstream therapy) are warranted.¹ There are strong indications that loss of proteostatic control in cardiomyocytes represents an important substrate for the development and progression of AF.³ The present study shows that HDAC6-induced α -tubulin deacetylation and microtubule disruption play a role in AF. Therefore, pharmacological inhibition of the major α -tubulin deacetylating enzyme HDAC6 represents a potentially promising target for upstream therapy. Because tubacin is not suitable for in vivo studies,¹⁸ other HDAC6 inhibitors such as tubastatin A and ACY-1215 have been developed and show beneficial effects in mice models for neurodegenerative diseases and cancer.^{18,42,43} In the present study, we provide the first evidence

for the efficacy of HDAC6 inhibitors in AF by demonstrating tubastatin A to protect against atrial remodeling in tachypaced dogs. Because the specific inhibition of HDAC6 has not been associated with any serious toxicity so far,³³ the present study suggests that HDAC6 is an interesting potential drug target for upstream therapy of AF.

Study Limitations

Our notion that HDAC6 activation contributes to human AF is based on the analysis of patients with lone AF or AF originating from mitral valve disease. Whether HDAC6 activation also contributes to AF of different origins needs to be established. Furthermore, although we obtained proof of concept of the beneficial effect of HDAC6 inhibition in AF, additional research should clarify whether HDAC6 inhibition also reverses the structural remodeling of cardiomyocytes in AF.

Sources of Funding

This study was supported by the Dutch Heart Foundation (2007B217 and 2009B024 to Dr Brundel, D. Zhang, and R.A.M. Meijering), the European Community, European Fund for Regional Development (Operationeel Programma Noord-Nederland 2007–2012, OP-EFRO to Dr Brundel, F. Hoogstra-Berends), TUBITAK (grant 108S375 to Drs Deniz, Durdu, and Akar), UMCG Imaging and Microscopy Center (NWO grants 40-00506-98-9021 and 175-010-2009-023), NWO VICI grant (865.10.012 to Dr Sibon), the Canadian Heart and Stroke Foundation (Dr Nattel), the Canadian Institutes of Health Research (MGP6957 and MOP44367; Dr Nattel), the Fondation Leducq (European-North American Atrial Fibrillation Research Alliance; Dr Nattel), and FRSQ-RSCV/HSFQ doctoral scholarship (A. Tadevosyan).

Disclosures

Dr Brundel is a scientific advisor and F. Hoogstra-Berends, who executed confocal measurements, is an employee of Nyken BV, a company holding intellectual property interests in heat shock protein targeting as a treatment in AF. The other authors report no conflicts.

References

1. Dobrev D, Carlsson L, Nattel S. Novel molecular targets for atrial fibrillation therapy. *Nat Rev Drug Discov*. 2012;11:275–291.
2. de Groot NM, Houben RP, Smeets JL, Boersma E, Schotten U, Schalij MJ, Crijns H, Allessie MA. Electropathological substrate of longstanding persistent atrial fibrillation in patients with structural heart disease: epicardial breakthrough. *Circulation*. 2010;122:1674–1682.
3. Meijering RAM, Zhang D, Hoogstra-Berends F, Henning RH, Brundel BJM. Loss of proteostatic control as a substrate for atrial fibrillation; a novel target for upstream therapy by heat shock proteins. *Front Card Electrophysiol*. 2012;3:36.
4. Haberland M, Montgomery RL, Olson EN. The many roles of histone deacetylases in development and physiology: implications for disease and therapy. *Nat Rev Genet*. 2009;10:32–42.
5. Balch WE, Morimoto RI, Dillin A, Kelly JW. Adapting proteostasis for disease intervention. *Science*. 2008;319:916–919.
6. Jenuwein T, Allis CD. Translating the histone code. *Science*. 2001;293:1074–1080.
7. Ausma J, Wijffels M, van Eys G, Koide M, Ramaekers F, Allessie M, Borgers M. Dedifferentiation of atrial cardiomyocytes as a result of chronic atrial fibrillation. *Am J Pathol*. 1997;151:985–997.
8. Thijssen VL, Ausma J, Gorza L, van der Velden HM, Allessie MA, Van Gelder IC, Borgers M, van Eys GJ. Troponin I isoform expression in human and experimental atrial fibrillation. *Circulation*. 2004;110:770–775.
9. Liu F, Levin MD, Petrenko NB, Lu MM, Wang T, Yuan LJ, Stout AL, Epstein JA, Patel VV. Histone-deacetylase inhibition reverses atrial arrhythmia inducibility and fibrosis in cardiac hypertrophy independent of angiotensin. *J Mol Cell Cardiol*. 2008;45:715–723.

10. Hubbert C, Guardiola A, Shao R, Kawaguchi Y, Ito A, Nixon A, Yoshida M, Wang XF, Yao TP. HDAC6 is a microtubule-associated deacetylase. *Nature*. 2002;417:455–458.
11. Haggarty SJ, Koeller KM, Wong JC, Grozinger CM, Schreiber SL. Domain-selective small-molecule inhibitor of histone deacetylase 6 (HDAC6)-mediated tubulin deacetylation. *Proc Natl Acad Sci USA*. 2003;100:4389–4394.
12. Matsuyama A, Shimazu T, Sumida Y, Saito A, Yoshimatsu Y, Seigneurin-Berny D, Osada H, Komatsu Y, Nishino N, Khochbin S, Horinouchi S, Yoshida M. In vivo destabilization of dynamic microtubules by HDAC6-mediated deacetylation. *EMBO J*. 2002;21:6820–6831.
13. Gupta MP, Samant SA, Smith SH, Shroff SG. HDAC4 and PCAF bind to cardiac sarcomeres and play a role in regulating myofilament contractile activity. *J Biol Chem*. 2008;283:10135–10146.
14. Gómez AM, Kerfant BG, Vassort G. Microtubule disruption modulates Ca(2+) signaling in rat cardiac myocytes. *Circ Res*. 2000;86:30–36.
15. Bush EW, McKinsey TA. Targeting histone deacetylases for heart failure. *Expert Opin Ther Targets*. 2009;13:767–784.
16. Brundel BJ, Shiroshita-Takeshita A, Qi X, Yeh YH, Chartier D, van Gelder IC, Henning RH, Kampinga HH, Nattel S. Induction of heat shock response protects the heart against atrial fibrillation. *Circ Res*. 2006;99:1394–1402.
17. Ke L, Qi XY, Dijkhuis AJ, Chartier D, Nattel S, Henning RH, Kampinga HH, Brundel BJ. Calpain mediates cardiac troponin degradation and contractile dysfunction in atrial fibrillation. *J Mol Cell Cardiol*. 2008;45:685–693.
18. Butler KV, Kalin J, Brochier C, Vistoli G, Langley B, Kozikowski AP. Rational design and simple chemistry yield a superior, neuroprotective HDAC6 inhibitor, tubastatin A. *J Am Chem Soc*. 2010;132:10842–10846.
19. Bradner JE, Mak R, Tanguturi SK, et al. Chemical genetic strategy identifies histone deacetylase 1 (HDAC1) and HDAC2 as therapeutic targets in sickle cell disease. *PNAS*. 2010;107:12617–12622.
20. Lavu S, Boss O, Elliott PJ, Lambert PD. Sirtuins—novel therapeutic targets to treat age-associated diseases. *Nat Rev Drug Discov*. 2008;7:841–853.
21. den Hoed M, Eijgelsheim M, Esko T, Brundel BJ, Peal DS, Evans DM, Nolte IM, Segrè AV, Holm H, Handsaker RE, Westra H, Johnson T, Isaacs A, Yang J, Lundby A, Zhao JH, Kim YJ, Go MJ, Almgren P, Bochud M, Boucher G, Cornelis MC, Gudbjartsson D, Hadley D, van der Harst P, Hayward C, den Heijer M, Igl W, Jackson AU, Kutalik Z, Luan J, Kemp JP, Kristiansson K, Ladenvall C, Lorentzon M, Montasser ME, Njajou OT, O'Reilly PF, Padmanabhan S, St. Pourcain B, Rankinen T, Salo P, Tanaka T, Timpson NJ, Vitart V, Waite L, Wheeler W, Zhang W, Draisma HH, Feitosa MF, Kerr KF, Lind PA, Mihailov E, Onland-Moret NC, Song C, Weedon MN, Xie W, Yengo L, Absher D, Albert CM, Alonso A, Arking DE, de Bakker PI, Balkau B, Barlassina C, Benaglio P, Bis JC, Bouatia-Naji N, Brage S, Chanock SJ, Chines PS, Chung M, Darbar D, Dina C, Dörr M, Elliott P, Felix SB, Fischer K, Fuchsberger C, de Geus EJ, Goyette P, Gudnason V, Harris TB, Hartikainen AL, Havulinna AS, Heckbert SR, Hicks AA, Hofman A, Holeywijn S, Hoogstra-Berends F, Hottenga JJ, Jensen MK, Johansson A, Junttila J, Kääb S, Kanon B, Ketkar S, Khaw KT, Knowles JW, Kooner AS, Kors JA, Kumari M, Milani L, Laiho P, Lakatta EG, Langenberg C, Leusink M, Liu Y, Luben RN, Lunetta KL, Lynch SN, Markus MR, Marques-Vidal P, Mateo Leach I, McArdle WL, McCarroll SA, Medland SE, Miller KA, Montgomery GW, Morrison AC, Müller-Nurasyid M, Navarro P, Nelis M, O'Connell JR, O'Donnell CJ, Ong KK, Newman AB, Peters A, Polasek O, Pouta A, Pramstaller PP, Psaty BM, Rao DC, Ring SM, Rossin EJ, Rudan D, Sanna S, Scott RA, Sehmi JS, Sharp S, Shin JT, Singleton AB, Smith AV, Soranzo N, Spector TD, Stewart C, Stringham HM, Tarasov KV, Uitterlinden AG, Vandenput L, Hwang SJ, Whitfield JB, Wijmenga C, Wild SH, Willemsen G, Wilson JF, Witteman JC, Wong A, Wong Q, Jamshidi Y, Zitting P, Boer JM, Boomsma DI, Borecki IB, van Duijn CM, Ekelund U, Forouhi NG, Froguel P, Hingorani A, Ingelsson E, Kivimäki M, Kronmal RA, Kuh D, Lind L, Martin NG, Oostra BA, Pedersen NL, Quertermous T, Rotter JJ, van der Schouw YT, Verschuren WM, Walker M, Albanes D, Arnar DO, Assimes TL, Bandinelli S, Boehnke M, de Boer RA, Bouchard C, Caulfield WL, Chambers JC, Curhan G, Cusi D, Eriksson J, Ferrucci L, van Gilst WH, Glorio N, de Graaf J, Groop L, Gyllenstein U, Hsueh WC, Hu FB, Huikuri HV, Hunter DJ, Iribarren C, Isomaa B, Jarvelin MR, Julia A, Kähönen M, Kiemeny LA, van der Klauw MM, Kooner JS, Kraft P, Iacoviello L, Lehtimäki T, Lokki ML, Mitchell BD, Navis G, Nieminen MS, Ohlsson C, Poulter NR, Qi L, Raitakari OT, Rimm EB, Rioux JD, Rizzi F, Rudan I, Salomaa V, Sever PS, Shields DC, Shuldiner AR, Sinisalo J, Stanton AV, Stolk RP, Strachan DP, Tardif JC, Thorsteinsdóttir U, Tuomilehto J, van Veldhuisen DJ, Virtamo J, Viikari J, Vollenweider P, Waechter G, Widen E, Cho YS, Olsen JV, Visscher PM, Willer C, Franke L, Erdmann J, Thompson JR, Pfeuffer A, Sotoodehnia N, Newton-Cheh C, Ellinor PT, Stricker BH, Metspalu A, Perola M, Beckmann JS, Smith GD, Stefansson K, Wareham NJ, Munroe PB, Sibon OC, Milan DJ, Snieder H, Samani NJ, Loos RJ; Global BPgen Consortium; CARDIoGRAM Consortium; PR GWAS Consortium; QRS GWAS Consortium; QT-IGC Consortium; CHARGE-AF Consortium. Identification of heart rate-associated loci and their effects on cardiac conduction and rhythm disorders. *Nat Genet*. 2013;45:621–631.
22. Zhang D, Ke L, Mackovicova K, Van Der Want JJ, Sibon OC, Tanguay RM, Morrow G, Henning RH, Kampinga HH, Brundel BJ. Effects of different small HSPB members on contractile dysfunction and structural changes in a *Drosophila melanogaster* model for atrial fibrillation. *J Mol Cell Cardiol*. 2011;51:381–389.
23. Lemon DD, Horn TR, Cavasin MA, Jeong MY, Haubold KW, Long CS, Irwin DC, McCune SA, Chung E, Leinwand LA, McKinsey TA. Cardiac HDAC6 catalytic activity is induced in response to chronic hypertension. *J Mol Cell Cardiol*. 2011;51:41–50.
24. Caron JM, Jones AL, Kirschner MW. Autoregulation of tubulin synthesis in hepatocytes and fibroblasts. *J Cell Biol*. 1985;101(pt 1):1763–1772.
25. Friedman JR, Webster BM, Mastrorade DN, Verhey KJ, Voeltz GK. ER sliding dynamics and ER-mitochondrial contacts occur on acetylated microtubules. *J Cell Biol*. 2010;190:363–375.
26. Zilberman Y, Ballestrin C, Carramusa L, Mazitschek R, Khochbin S, Bershadsky A. Regulation of microtubule dynamics by inhibition of the tubulin deacetylase HDAC6. *J Cell Sci*. 2009;122(pt 19):3531–3541.
27. Nam HJ, Kang JK, Kim SK, Ahn KJ, Seok H, Park SJ, Chang JS, Pothoulakis C, Lamont JT, Kim H. *Clostridium difficile* toxin A decreases acetylation of tubulin, leading to microtubule depolymerization through activation of histone deacetylase 6, and this mediates acute inflammation. *J Biol Chem*. 2010;285:32888–32896.
28. Billger M, Wallin M, Karlsson JO. Proteolysis of tubulin and microtubule-associated proteins 1 and 2 by calpain I and II: difference in sensitivity of assembled and disassembled microtubules. *Cell Calcium*. 1988;9:33–44.
29. Brundel BJ, Ausma J, van Gelder IC, Van der Want JJ, van Gilst WH, Crijns HJ, Henning RH. Activation of proteolysis by calpains and structural changes in human paroxysmal and persistent atrial fibrillation. *Cardiovasc Res*. 2002;54:380–389.
30. Verdel A, Curtet S, Brocard MP, Rousseaux S, Lemerrier C, Yoshida M, Khochbin S. Active maintenance of mHDA2/mHDAC6 histone-deacetylase in the cytoplasm. *Curr Biol*. 2000;10:747–749.
31. Kawaguchi Y, Kovacs JJ, McLaurin A, Vance JM, Ito A, Yao TP. The deacetylase HDAC6 regulates aggresome formation and cell viability in response to misfolded protein stress. *Cell*. 2003;115:727–738.
32. Iwata A, Riley BE, Johnston JA, Kopito RR. HDAC6 and microtubules are required for autophagic degradation of aggregated huntingtin. *J Biol Chem*. 2005;280:40282–40292.
33. Witt O, Deubzer HE, Milde T, Oehme I. HDAC family: what are the cancer relevant targets? *Cancer Lett*. 2009;277:8–21.
34. Boyault C, Sadoul K, Pabion M, Khochbin S. HDAC6, at the crossroads between cytoskeleton and cell signaling by acetylation and ubiquitination. *Oncogene*. 2007;26:5468–5476.
35. Kolodney MS, Elson EL. Contraction due to microtubule disruption is associated with increased phosphorylation of myosin regulatory light chain. *Proc Natl Acad Sci USA*. 1995;92:10252–10256.
36. Galli A, DeFelice LJ. Inactivation of L-type Ca channels in embryonic chick ventricle cells: dependence on the cytoskeletal agents colchicine and taxol. *Biophys J*. 1994;67:2296–2304.
37. Leach RN, Desai JC, Orchard CH. Effect of cytoskeleton disruptors on L-type Ca channel distribution in rat ventricular myocytes. *Cell Calcium*. 2005;38:515–526.
38. North BJ, Marshall BL, Borra MT, Denu JM, Verdin E. The human Sir2 ortholog, SIRT2, is an NAD⁺-dependent tubulin deacetylase. *Mol Cell*. 2003;11:437–444.
39. Yang T, Sauve AA. NAD metabolism and sirtuins: metabolic regulation of protein deacetylation in stress and toxicity. *AAPS J*. 2006;8:E632–E643.
40. Yang H, Yang T, Baur JA, Perez E, Matsui T, Carmona JJ, Lamming DW, Souza-Pinto NC, Bohr VA, Rosenzweig A, de Cabo R, Sauve AA, Sinclair DA. Nutrient-sensitive mitochondrial NAD⁺ levels dictate cell survival. *Cell*. 2007;130:1095–1107.
41. Riviello MA, Brochier C, Willis DE, Walker BA, D'Annibale MA, McLaughlin K, Siddiq A, Kozikowski AP, Jaffrey SR, Twiss JL, Ratan RR, Langley B. HDAC6 is a target for protection and regeneration following injury in the nervous system. *Proc Natl Acad Sci U S A*. 2009;106:19599–19604.
42. Santo L, Hideshima T, Kung AL, Tseng JC, Tamang D, Yang M, Jarpe M, van Duzer JH, Mazitschek R, Ogier WC, Cirstea D, Rodig S, Eda

H, Scullen T, Canavese M, Bradner J, Anderson KC, Jones SS, Raje N. Preclinical activity, pharmacodynamic, and pharmacokinetic properties of a selective HDAC6 inhibitor, ACY-1215, in combination with bortezomib in multiple myeloma. *Blood*. 2012;119:2579–2589.

43. d'Ydewalle C, Krishnan J, Chiheb DM, Van Damme P, Irobi J, Kozikowski AP, Vanden Berghe P, Timmerman V, Robberecht W, Van Den Bosch L. HDAC6 inhibitors reverse axonal loss in a mouse model of mutant HSPB1-induced Charcot-Marie-Tooth disease. *Nat Med*. 2011;17:968–974.

CLINICAL PERSPECTIVE

Drugs currently used in atrial fibrillation (AF) have limited efficacy in preventing remodeling of cardiac tissue. Thus, pharmacological approaches preventing or limiting such remodeling, which is considered a prime substrate for the promotion of AF, are warranted (upstream therapy). There are strong indications that a loss of normal protein homeostasis in cardiomyocytes contributes significantly to the substrate for the development and progression of AF. Our present study identifies histone deacetylase-6 (HDAC6)-induced deacetylation of α -tubulin and subsequent microtubule disruption as a critical step in the development of a substrate for AF. Consequently, inhibitors of HDAC6 represent promising drug candidates for upstream therapy. Because the HDAC6 inhibitor we used in model systems, tubacin, is not suitable for in vivo studies, alternative inhibitors such as tubastatin A and ACY-1215 have recently been developed. These inhibitors show beneficial effects in mice models of neurodegenerative diseases and cancer. In the present study, we provide the first evidence for the in vivo efficacy of such HDAC6 inhibitors in AF by demonstrating that tubastatin A protects against atrial remodeling in tachypaced dogs. Specific inhibition of HDAC6 has not been associated with any serious toxicity so far, and clinical trials are currently recruiting for phase 1/2 studies. Thus, should these trials substantiate the lack of toxicity of HDAC6 inhibitors in humans, our present study suggests that these drugs represent interesting candidates to be tested for upstream therapy in human AF.

Supplemental Data

Supplemental Methods:

Canine model

Dogs were anesthetized with acepromazine (0.07 mg/kg i.m.), ketamine (5.3 mg/kg i.v.), diazepam (0.25 mg/kg, i.v.), and isoflurane (1.5%), intubated, and ventilated. One bipolar pacing lead was fixed into the right atrial (RA) appendage via the left jugular vein under fluoroscopic guidance. The tip was connected to a programmable pacemaker (Star Medical, Japan). Osmotic pumps (2 ml with one-week delivery; Alzet, Cupertino, CA) filling with either 50% DMSO alone (for sham and ATP group) or tubastatin A in 50% DMSO were implanted subcutaneously. For ATP and ATP + tubastatin A groups, the pacemakers were turned on 24 hours after surgery to stimulate the RA at 600 bpm for 7 successive days. The ECG was checked daily to ensure AF during pacing. At the end of the study, all dogs were anesthetized with morphine (2mg/kg s.c.) and α -chloralose (120mg/kg i.v. bolus followed by 29.25mg/kg/hr i.v. infusion), intubated and ventilated. Body temperature was maintained at 37°C. After midline sternotomy, the pericardium was opened and 2 bipolar electrodes were fixed to the RA appendage (one for pacing, one for signal recording). For AF-induction, the RA was paced at 50 Hz for 3-10 seconds. A total of 5-10 AF episodes were recorded to calculate the mean AF duration in each dog. An AF episode >30 minutes was considered sustained, and the electrophysiological study was terminated. Cardioversion was avoided to prevent tissue damage, which precludes further cellular and molecular studies. In one sham dog, substantial electrophysiological derangements were observed at terminal study, including significant sinus node dysfunction and prolonged AF, as well as signs of senescence. These results could not be predicted at study initiation, because electrophysiological data were not obtained prior to the terminal study. The results of that dog were excluded for all analyses because of presumed underlying heart disease. To avoid bias due to

exclusion from the sham group of a dog with prolonged AF, we also excluded from analysis the results of individual dogs with the longest-lasting AF in each of the other 2 groups (ATP+vehicle and ATP+tubastatin A).

Atrial cardiomyocyte isolation

After electrophysiological study, the heart was excised and immersed in oxygen-saturated Tyrode solution (in mmol/L NaCl 136, KCl 5.4, MgCl₂ 1, CaCl₂ 2, NaH₂PO₄ 0.33, HEPES 5 and dextrose 10, pH 7.35 by NaOH). The left atrium (LA) was isolated from the heart with intact blood supply. The left circumflex coronary artery was cannulated and perfused with Ca²⁺-containing (1.8 mmol/L) Tyrode solution for 10 minutes, followed by Ca²⁺-free Tyrode-solution perfusion for another 10 minutes. All leaking branches were ligated. The tissue was then perfused with Ca²⁺-free Tyrode-solution containing 150 U/mL collagenase (Worthington, type II) and 0.1% bovine serum albumin (BSA) for 60 minutes. Digested LA-tissue was harvested and carefully stirred. Isolated cells were centrifuged (500 rpm, 3 minutes) to separate cardiomyocytes from fibroblasts. Cardiomyocytes were stored in Tyrode-solution containing 200 μmol/L Ca²⁺ for Ca²⁺-imaging studies and in Kraft-Bruhe solution (in mmol/L: K-glutamate 100, K-aspartate 10, KCl 25, KH₂PO₄ 10, MgSO₄ 2, taurine 20, EGTA 0.5, glucose 20, HEPES 5, and 1% BSA) for patch clamping.

Cardiomyocyte Ca²⁺ imaging and cellular contractility assessment

Isolated cardiomyocytes were stimulated at 1 Hz and all measurements were performed at 35±2°C. Cell-Ca²⁺ recording was obtained as previously described with the use of Indo-1 AM.¹ Cells were exposed to UV light (wave-length 340 nm) and the exposure was controlled with an electronic shutter to minimize photo bleaching. Emitted light was reflected into a spectral separator, passed through parallel filters at 400 and 500 nm (±10 nm), detected by matched photomultiplier tubes, and electronically filtered at 60 Hz. Background fluorescence was removed by adjusting the 400- and

500-nm channels to 0 over an empty field of view near the cell. Fluorescence signal ratios (R) were recorded and converted to $[Ca^{2+}]_i$ following the equation developed by Grynkiewicz et al.² :

$$[Ca^{2+}]_i = K_d \beta [(R - R_{min}) / (R_{max} - R)]$$

where β is the ratio of the 500-nm signals at very low and saturating $[Ca^{2+}]_i$. Intracellular K_d for *indo-1* was 844 nM. Cell and sarcomere contractility was detected by automatic edge-detection and 5 successive beats were averaged for each measurement.

Cell Electrophysiology Recordings

Borosilicate glass electrodes (Sutter Instruments, Novato, CA) filled with pipette solution were connected to a patch-clamp amplifier (Axopatch 200A, Axon Instruments, Foster City, CA). Electrodes had tip resistances of 2-4 M Ω . For perforated-patch recording, nystatin-free intracellular solution was placed in the tip of the pipette by capillary action (~30 s), then pipettes were back-filled with nystatin-containing (600 μ g/mL) pipette solution. Data were sampled at 5 kHz and filtered at 1 kHz. Whole cell currents are expressed as densities (pA/pF). Junction potentials between bath and pipette solutions averaged 10.5 mV and were corrected for APs only. KB-solution contained (mmol/L): KCl 20, KH₂PO₄ 10, dextrose 10, mannitol 40, L-glutamic acid 70, β -OH-butyric acid 10, taurine 20, and EGTA 10 and 0.1% BSA (pH 7.3, KOH). Tyrode's solution contained (mmol/L): NaCl 136, CaCl₂ 1.8, KCl 5.4, MgCl₂ 1, NaH₂PO₄ 0.33, dextrose 10, and HEPES 5, titrated to pH 7.3 with NaOH. The pipette solution for AP-recording contained (mmol/L) GTP 0.1, potassium-aspartate 110, KCl 20, MgCl₂ 1, MgATP 5, HEPES 10, sodium-phosphocreatine 5, and EGTA 0.005 (pH 7.4, KOH). The extracellular solution for Ca²⁺-current (I_{Ca}) measurement contained (mmol/L): tetraethylammonium-chloride 136, CsCl 5.4, MgCl₂ 1, CaCl₂ 2, NaH₂PO₄ 0.33, dextrose 10, and HEPES 5 (pH 7.4, CsOH). Niflumic acid (50 μ mol/L) was added to inhibit Ca²⁺ dependent Cl⁻-current, and 4-aminopyridine (2 mmol/L) to suppress I_{to} . The pipette solution for I_{Ca} -recording contained (mmol/L)

CsCl 120, tetraethylammonium-chloride 20, MgCl₂ 1, EGTA 10, Mg-ATP 5, HEPES 10, and Li-GTP 0.1 (pH 7.4, CsOH).

Slot Blotting and Western Blotting

Slot blot analysis was performed as described previously.³ In short, frozen RAA and LAA of patients, pre-pupae of *Drosophila* or HL-1 cardiomyocytes were lysed in RIPA buffer. Protein concentration was measured according to the Bradford method (Bio-Rad, The Netherlands). Equal amounts (10µg) of heat-denatured protein were used for Western blotting or spotted on nitrocellulose membranes (Stratagene) by the use of a slot blot apparatus (Bio-Rad) and checked by staining with Ponceau S solution (Sigma). After blocking with skim milk, membranes were incubated with primary antibody against acetyl lysine (Cell Signaling), acetyl Histone 3 (Cell Signaling), or GAPDH (Fitzgerald), followed by incubation with secondary HRP-conjugated anti-rabbit antibody (Amersham). Signals were detected by the ECL-detection method (Amersham) and quantified by densitometry (Syngene Genetools).

In vitro calpain mediated α -tubulin degradation assay

To measure α -tubulin degradation by calpain *in vitro*, α -tubulin was isolated from HL-1 cardiomyocytes by immunoprecipitation with non-denaturing lysis buffer (Tris HCl pH 8, 137 mmol/L NaCl, 10% glycerol, 1% Nonidet P-40 (NP-40), and 2 mmol/L EDTA). A/G beads (Santa Cruz) were coated with α -tubulin antibody (Sigma) to pull down α -tubulin from HL-1 cardiomyocyte lysate. To detach α -tubulin from the beads, the beads were incubated with elution buffer (0.2mol/L glycine pH2.5) at room temperature for 10 min. After centrifugation, beads were removed and the eluate containing α -tubulin was transferred to a new tube, followed by adjustment to physiological pH by adding neutralization buffer (1mol/L Tris PH9.5, 1/10 v/v of elution buffer). To detect degradation of

α -tubulin by calpain, calpain I (Merck/Calbiochem) was incubated with the same amount of α -tubulin eluate in reaction buffer (PBS with 2mmol/L CaCl_2) for 1 hour at room temperature. After incubation, loading buffer (10% SDS, 50% glycerol, 0.33mol/L Tris HCl pH=6.8, 10% beta-mercaptoethanol, 0.05% bromophenol blue) was added to the tube followed by 5 min boiling. Western blot analysis was used to detect α -tubulin.

HDAC activity measurements

The overall HDAC activity was measured by utilizing a fluorimetric HDAC activity assay kit (Sigma) according to the manufacturer's instructions. Briefly, normal or tachypaced HL-1 cardiomyocytes or atrial tissue samples were lysed in non-denaturing buffer (CellLytic™ MT Cell Lysis Reagent, Sigma). Protein concentrations were determined by Bio-Rad Protein Assay Kit (Bio-Rad). Fluorescence was measured with a fluorimeter (Bio-tek instruments FLx800) at 360nm excitation and 460nm emission wavelength. To test efficiency of HDAC inhibitors in HL-1 cardiomyocytes, lysates were incubated with the HDAC inhibitors as described in Table 1. Blank samples and samples with HeLa cell nuclear extracts were used as negative and positive controls, respectively.

Supplemental Figures

Figure S1

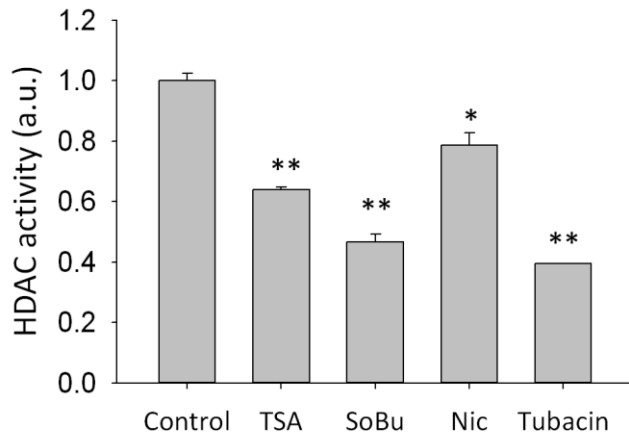


Figure S2

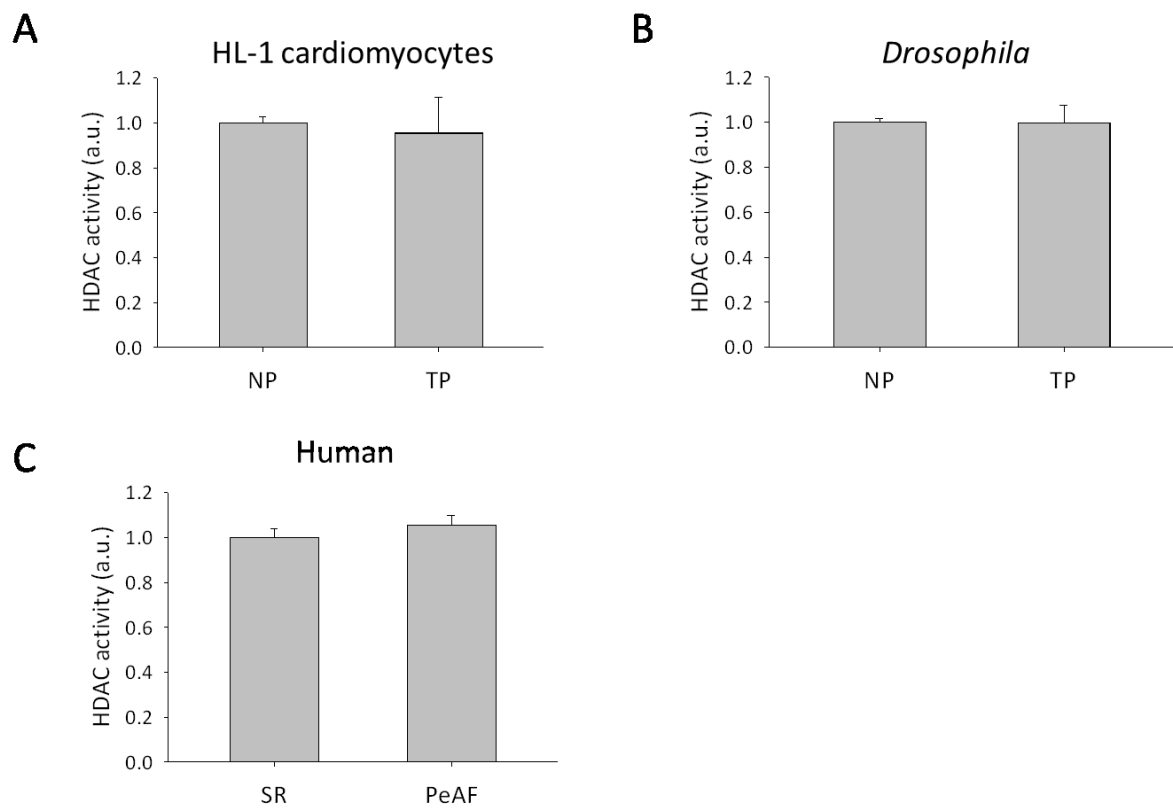


Figure S3

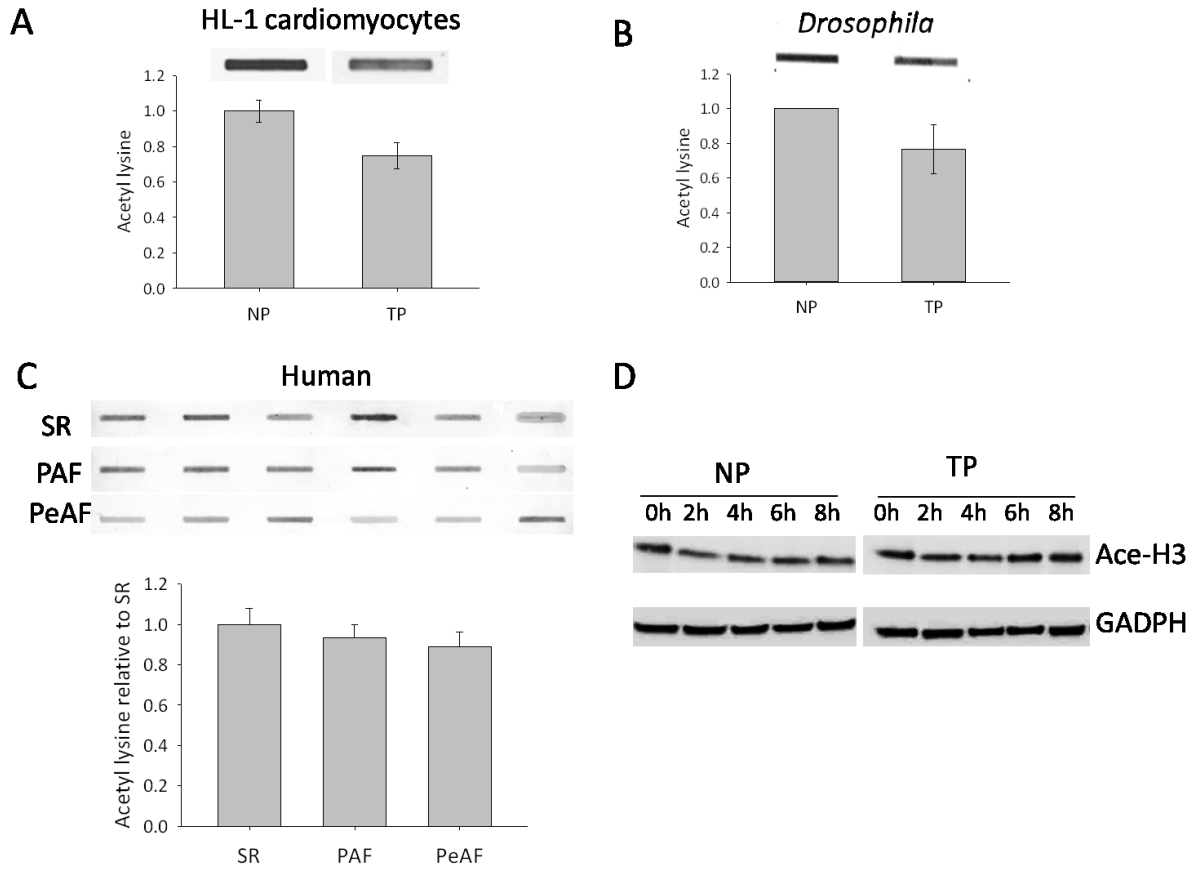


Figure S4

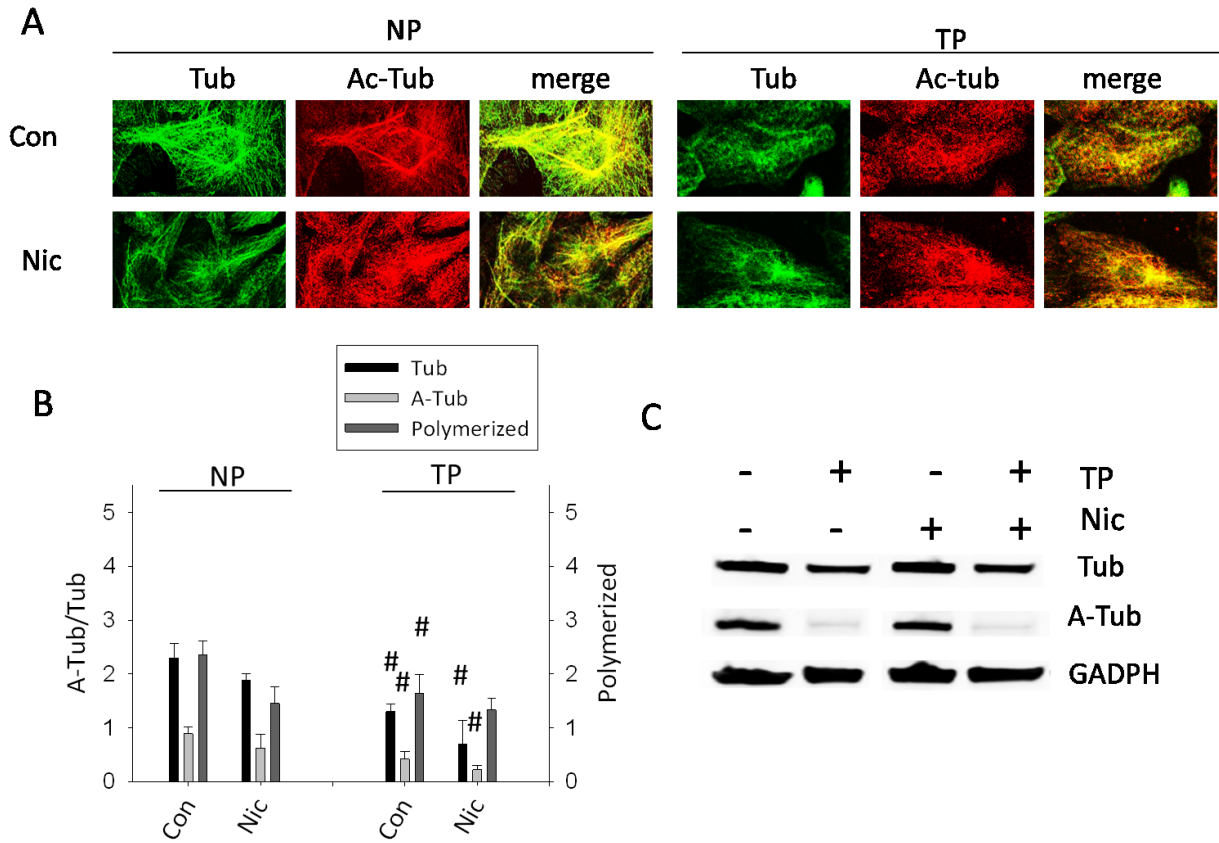


Figure S5

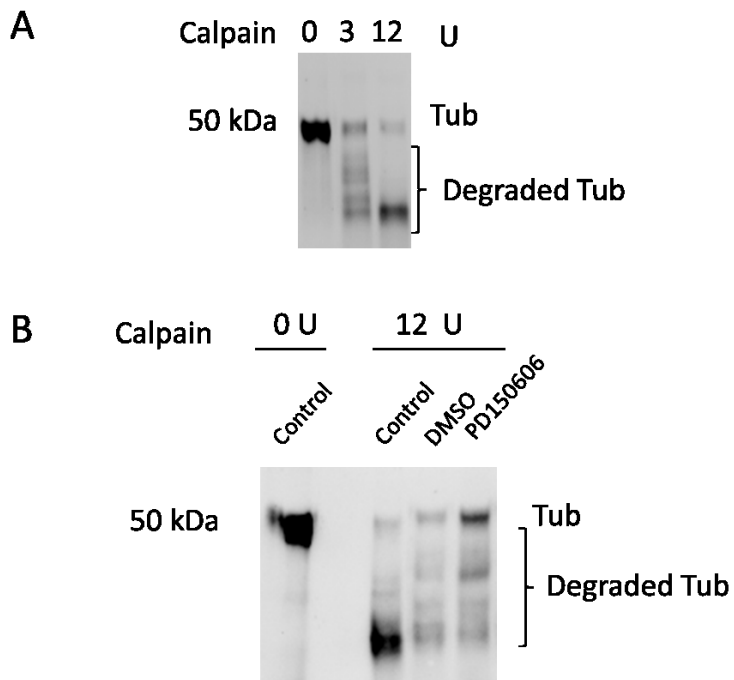


Figure S6

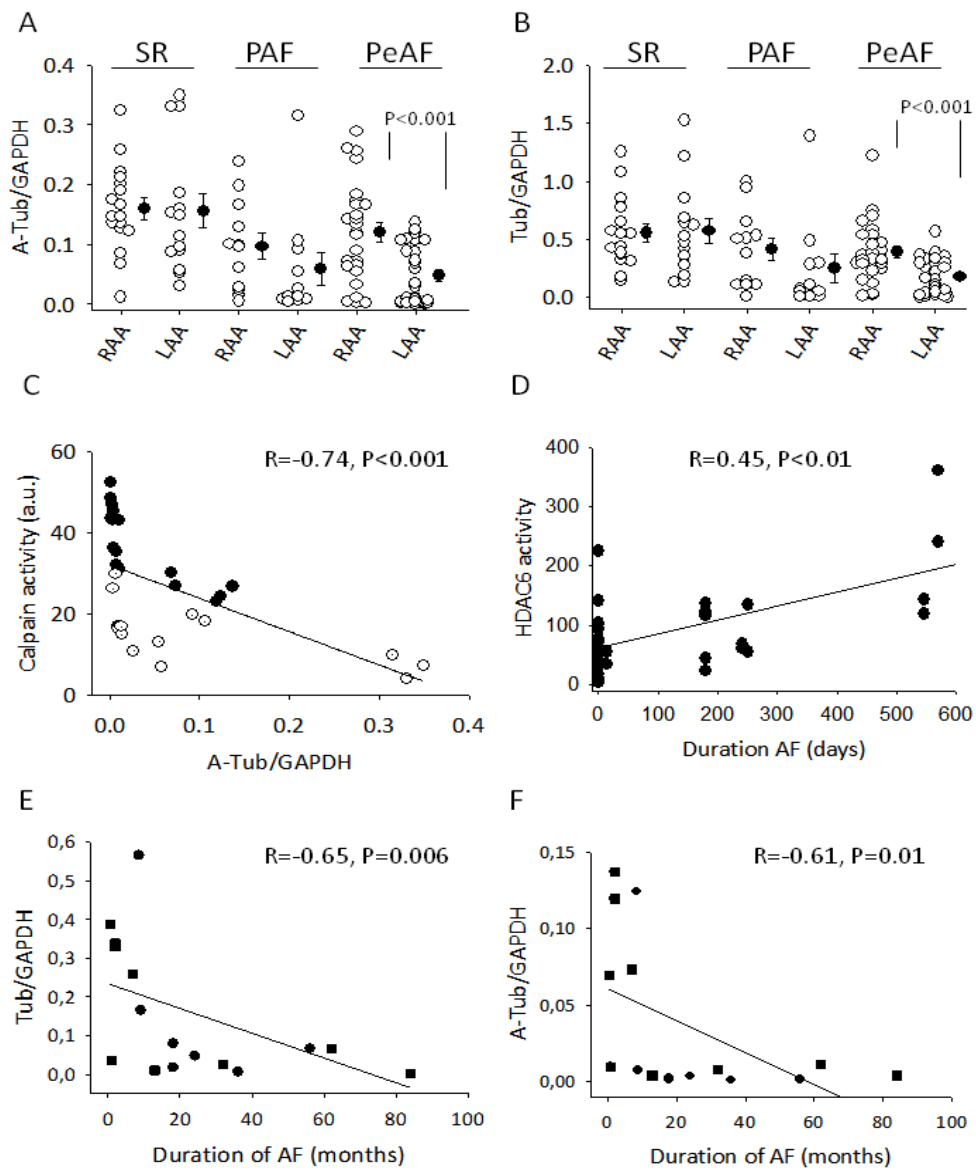
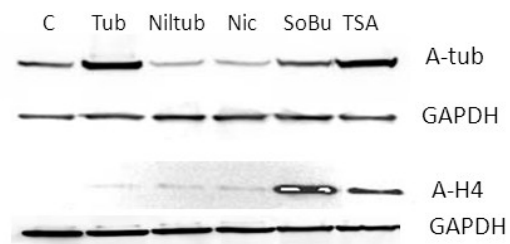


Figure S7



Supplemental Figure Legends

Figure S1: *Efficacy of HDAC inhibitors to reduce overall HDAC activity in Drosophila.* All the HDAC inhibitors significantly reduced HDAC activity at the concentrations used as described in Table 1.

* $P < 0.05$ vs control, ** $P < 0.01$ vs control (without HDAC inhibitor).

Figure S2: *No significant changes in overall HDAC activity after tachypacing of HL-1 cardiomyocytes, Drosophila and in clinical AF.* Overall HDAC activity was tested using the HDAC activity assay kit. No changes in total HDAC activity were observed between (A) normal (NP) and tachypaced (TP) HL-1 cardiomyocytes and (B) *Drosophila* and (C) between patients in normal sinus rhythm (SR, n=6) and permanent AF (PeAF, n=6). Experiments were performed in at least in duplicate series.

Figure S3: *No significant changes in overall acetyl lysine and acetyl histone H3 levels after tachypacing of HL-1 cardiomyocytes, Drosophila or during clinical AF.* Insets in panel A-C are representative slot blots showing overall lysine levels in normal (NP) or tachypaced (TP) (A) HL-1 cardiomyocytes, (B) *Drosophila* and (C) human paroxysmal (PAF), permanent AF (PeAF) and controls in sinus rhythm (SR). Graphs show quantified data demonstrating the absence of significant changes between the groups as indicated. D) Western blot showing no significant differences in acetyl histone H3K9 (Ace-H3) levels between NP and TP HL-1 cardiomyocytes. All experiments were performed in at least duplicate series.

Figure S4: *Nicotinamide does not prevent tachypacing-induced deacetylation of α -tubulin and depolymerization of microtubules.* A) Typical example of an immunofluorescent staining of α -tubulin (green), acetyl α -tubulin (red) in normal paced (NP) and tachypaced (TP) HL-1 cardiomyocytes. Tachypacing with or without nicotinamide treatment, induces depolymerization of microtubules (yellow) which is not prevented by pre-treatment with nicotinamide. B) Quantification of α -tubulin (Tub), acetylated α -tubulin (A-Tub) and amount of polymerized tubulin (microtubules) after NP and

TP. TP significantly reduced the amount of Tub, A-Tub and and polymerized α -tubulin, which was not prevented by nicotinamide (100-250 cells per condition). C) Representative Western blot showing tachypacing-induced reductions in total α -tubulin and acetyl tubulin which was not prevented by nicotinamide pretreatment. # $P < 0.01$ vs Control NP.

Figure S5: *Depolymerized α -tubulin is degraded by calpain in vitro.* A) Depolymerized α -tubulin was incubated with increasing amounts of calpain, which resulted in accelerated degradation of α -tubulin. B) Calpain-induced α -tubulin degradation was attenuated by the calpain inhibitor PD150606.

Figure S6: *Patients with AF reveal reduced levels of acetylated and total α -tubulin in LAA.* A) Quantification of acetyl α -tubulin and B) α -tubulin in RAA and LAA. In patients with PeAF, LAAs show significant reductions in acetyl and total α -tubulin compared to RAAs. (RAA, n=16 for SR, n=12 for PAF, n=25 for PeAF; LAA, n=14 for SR, n=11 for PAF, n=27 for PeAF) C) Significant inverse correlation between tissue calpain activity and the amount of acetyl α -tubulin in LAA. (●) represents PAF (n=11), (○) represents PeAF (n=16), (o) represents SR (n=3). D) Significant correlation between duration of PeAF and HDAC6 activity. Included are RAA and LAA of SR patients (n=12) and PeAF (n=7). E) and F) Significant inverse correlation between duration of AF and expression of α -tubulin (E) and acetyl α -tubulin (F) in LAA of patients with lone PeAF (●, n=7) or PeAF with mitral valve disease (■, n=9).

Figure S7: *Pan HDAC inhibitors TSA and sodium butyrate, but not tubacin, induce histone H4 acetylation, while all three drugs do acetylate α -tubulin.* Representative Western blots showing the acetylated α -tubulin and histone H4 levels (A-H4) in HL-1 cardiomyocytes treated with various HDAC inhibitors as indicated. Concentration of drugs used as mentioned in Table 1 and for niltubacin 1 μ M was used.

Movie S1: *Time-lapse movie shows CaT after 8 hours normal pacing (1Hz) of HL-1 cardiomyocytes.* Images were acquired at 2 ms intervals.

Movie S2: Time-lapse movie shows CaT after 8 hours tachypacing (4Hz) of HL-1 cardiomyocytes. Images were acquired at 2 ms intervals.

Movie S3: Time-lapse movie shows CaT after 8 hours tachypacing (4Hz) of HL-1 cardiomyocytes pretreated with TSA. Images were acquired at 2 ms intervals.

Movie S4: Time-lapse movie shows CaT after 8 hours tachypacing (4Hz) of HL-1 cardiomyocytes pretreated with Sodiumbutyrate. Images were acquired at 2 ms intervals.

Movie S5: Time-lapse movie shows CaT after 8 hours tachypacing (4Hz) of HL-1 cardiomyocytes pretreated with Nicotinamide. Images were acquired at 2 ms intervals.

Movie S6: Time-lapse movie shows CaT after 8 hours tachypacing (4Hz) of HL-1 cardiomyocytes pretreated with Tubacin. Images were acquired at 2 ms intervals.

Movie S7: Time-lapse movie shows CaT after 8 hours tachypacing (4Hz) of HL-1 cardiomyocytes pretreated with Niltubacin. Images were acquired at 2 ms intervals.

Movie S8: Time-lapse movie shows heart wall contractions of an early pupa of a W1118 genetic background before tachypacing, during tachypacing (4Hz) **Movie S9** and after tachypacing **Movie S10**.

Movie S11: Time-lapse movie shows heart wall contractions of an early pupa of a W1118 genetic background pretreated with TSA before tachypacing, and after tachypacing **Movie S12**.

Movie S13: Time-lapse movie shows heart wall contractions of an early pupa of a W1118 genetic background pretreated with Sodiumbutyrate before tachypacing, and after tachypacing **Movie S14**.

Movie S15: Time-lapse movie shows heart wall contractions of an early pupa of a W1118 genetic background pretreated with Nicotinamide before tachypacing, and after tachypacing **Movie S16**.

Movie S17: Time-lapse movie shows heart wall contractions of an early pupa of a W1118 genetic background pretreated with Tubacin before tachypacing, and after tachypacing **Movie S18**.

Supplemental References

1. Nishida K, Chiba K, Iwasaki YK, et al. Atrial fibrillation-associated remodeling does not promote atrial thrombus formation in canine models. *Circ Arrhythm Electrophysiol*. 2012;5(6):1168-1175.
2. Grynkiewicz G, Poenie M, Tsien RY. A new generation of Ca²⁺ indicators with greatly improved fluorescence properties. *J Biol Chem*. 1985;260(6):3440-3450.
3. Brundel BJM, Van Gelder IC, Henning RH, et al. Ion channel remodeling is related to intra-operative atrial refractory periods in patients with paroxysmal and persistent atrial fibrillation. *Circulation*. 2001;103:684-690.

Activation of Histone Deacetylase-6 Induces Contractile Dysfunction Through Derailment of α -Tubulin Proteostasis in Experimental and Human Atrial Fibrillation

Deli Zhang, Chia-Tung Wu, XiaoYan Qi, Roelien A.M. Meijering, Femke Hoogstra-Berends, Artavazd Tadevosyan, Gunseli Cubukcuoglu Deniz, Serkan Durdu, Ahmet Ruchan Akar, Ody C.M. Sibon, Stanley Nattel, Robert H. Henning and Bianca J.J.M. Brundel

Circulation. 2014;129:346-358; originally published online October 21, 2013;
doi: 10.1161/CIRCULATIONAHA.113.005300

Circulation is published by the American Heart Association, 7272 Greenville Avenue, Dallas, TX 75231
Copyright © 2013 American Heart Association, Inc. All rights reserved.
Print ISSN: 0009-7322. Online ISSN: 1524-4539

The online version of this article, along with updated information and services, is located on the
World Wide Web at:

<http://circ.ahajournals.org/content/129/3/346>

Data Supplement (unedited) at:

<http://circ.ahajournals.org/content/suppl/2013/10/21/CIRCULATIONAHA.113.005300.DC1.html>

Permissions: Requests for permissions to reproduce figures, tables, or portions of articles originally published in *Circulation* can be obtained via RightsLink, a service of the Copyright Clearance Center, not the Editorial Office. Once the online version of the published article for which permission is being requested is located, click Request Permissions in the middle column of the Web page under Services. Further information about this process is available in the [Permissions and Rights Question and Answer](#) document.

Reprints: Information about reprints can be found online at:
<http://www.lww.com/reprints>

Subscriptions: Information about subscribing to *Circulation* is online at:
<http://circ.ahajournals.org/subscriptions/>